© 2022. Published by The Company of Biologists Ltd | Disease Models & Mechanisms (2022) 15, dmm049387. doi:10.1242/dmm.049387

RESEARCH ARTICLE

Therapeutic potential of macrophage colony-stimulating factor in chronic liver disease

Sahar Keshvari[1,*], Berit Genz[1,2,*], Ngari Teakle[1], Melanie Caruso[1], Michelle F. Cestari[1], Omkar L. Patkar[1], Brian W. C. Tse[3], Kamil A. Sokolowski[3], Hilmar Ebersbach[4], Julia Jascur[4], Kelli P. A. MacDonald[2], Gregory Miller[5], Grant A. Ramm[2,6], Allison R. Pettit[1], Andrew D. Clouston[5,6], Elizabeth E. Powell[6,7], David A. Hume[1] and Katharine M. Irvine[1,‡]

ABSTRACT

Resident and recruited macrophages control the development and proliferation of the liver. We have previously shown in multiple species that treatment with a macrophage colony stimulating factor (CSF1)-Fc fusion protein initiated hepatocyte proliferation and promoted repair in models of acute hepatic injury in mice. Here, we investigated the impact of CSF1-Fc on resolution of advanced fibrosis and liver regeneration, using a non-resolving toxin-induced model of chronic liver injury and fibrosis in C57BL/6J mice. Co-administration of CSF1-Fc with exposure to thioacetamide (TAA) exacerbated inflammation consistent with monocyte contributions to initiation of pathology. After removal of TAA, either acute or chronic CSF1-Fc treatment promoted liver growth, prevented progression and promoted resolution of fibrosis. Acute CSF1-Fc treatment was also anti-fibrotic and pro-regenerative in a model of partial hepatectomy in mice with established fibrosis. The beneficial impacts of CSF1-Fc treatment were associated with monocyte-macrophage recruitment and increased expression of remodelling enzymes and growth factors. These studies indicate that CSF1-dependent macrophages contribute to both initiation and resolution of fibrotic injury and that CSF1-Fc has therapeutic potential in human liver disease.

KEY WORDS: Chronic liver disease, Liver regeneration, Fibrosis resolution, Inflammation, Macrophages, Thioacetamide, Mouse

INTRODUCTION

Fibrosis is a physiological response to acute and chronic tissue injury. In the developed world, 45% of all-cause mortality may be attributable to fibrotic disorders (Wynn, 2008). Chronic liver disease (CLD) and associated liver fibrosis, cirrhosis and its complications and hepatocellular carcinoma (HCC) affect more than 1.5 billion people and cause more than two million deaths each year (Asrani et al., 2019; Moon et al., 2020). Liver injury of any aetiology causes an inflammatory response leading to myofibroblast activation and collagen deposition (Wynn, 2008). Where the injury persists, ongoing extracellular matrix (ECM) deposition leads to disruption of the liver architecture, eventually leading to portal hypertension and loss of liver function characteristic of cirrhosis. Patients with cirrhosis are at high risk of life-threatening complications and HCC. Despite an active clinical trial pipeline (Lemoinne and Friedman, 2019), no anti-fibrotic therapies are available.

Liver fibrogenesis is a dynamic process that can be modulated by preventing progression or promoting resolution of fibrosis. Fibrosis may reverse in patients receiving successful antiviral therapy and in abstinent alcohol-induced cirrhosis patients (D'Ambrosio et al., 2012; Marcellin et al., 2013; Schuppan et al., 2018), but many patients with advanced fibrosis due to viral hepatitis or alcohol-induced cirrhosis progress despite removal of the primary stimulus (Schuppan et al., 2018). Fibrosis also complicates surgery in CLD patients (for example to remove a tumour) as it can also impair regeneration (Hackl et al., 2016; Krenzien et al., 2018).

Macrophages and monocytes contribute to both disease progression and resolution in CLD (Duffield et al., 2005; Irvine et al., 2019; Kisseleva and Brenner, 2021; Tacke, 2017). Inhibition of some macrophage functions (e.g. Wnt secretion, autophagy, phagocytosis) during disease progression can exacerbate fibrosis (Irvine et al., 2015; Lodder et al., 2015; Perugorria et al., 2018; Wan et al., 2020). During fibrosis resolution, macrophages may transition to a pro-repair phenotype, clearing damaged tissue, dampening inflammation and fibroblast activation, and producing growth and matrix remodelling factors that reduce fibrous tissue and restore liver architecture (Ramachandran et al., 2012). However, in contrast to the significant interest in macrophages as therapeutic targets to limit inflammation (Tacke, 2017), few therapeutic approaches to promote macrophage pro-regenerative functions have been explored (Barcena et al., 2019; Han et al., 2019; Wan et al., 2020).

Signalling through the macrophage colony-stimulating factor receptor (CSF1R) drives monocyte differentiation, proliferation and function (Hume et al., 2019). To test potential therapeutic applications in tissue repair, we generated a porcine CSF1-Fc fusion protein that has an extended circulating half-life compared with the native protein, and CSF1-Fc treatment promoted hepatocyte proliferation and liver growth in healthy mice, rats and pigs (Gow et al., 2014; Irvine et al., 2020; Sauter et al., 2016). Acute CSF1-Fc treatment increased liver macrophage content through both CCR2-dependent monocyte infiltration and resident macrophage proliferation (Gow et al., 2014; Stutchfield et al., 2015). CSF1R is

[1]Mater Research Institute, The University of Queensland, Translational Research Institute, Brisbane, Queensland 4102, Australia. [2]QIMR Berghofer Medical Research Institute, Brisbane, Queensland 4006, Australia. [3]Preclinical Imaging Facility, Translational Research Institute, Brisbane, Queensland 4102, Australia. [4]Novartis Institutes for Biomedical Research (NIBR), Fabrikstrasse 2, Novartis Campus, CH-4056 Basel, Switzerland. [5]Envoi Specialist Pathologists, Brisbane, Queensland 4059, Australia. [6]Faculty of Medicine, The University of Queensland, Brisbane, Queensland 4006, Australia. [7]Department of Gastroenterology and Hepatology, Princess Alexandra Hospital, Brisbane, Queensland 4102, Australia.
*These authors contributed equally to this work

‡Author for correspondence (Katharine.irvine@uq.edu.au)

S.K., 0000-0002-8116-8889; B.G., 0000-0002-8038-9815; M.C., 0000-0001-9159-5422; A.D.C., 0000-0002-9601-7952; K.M.I., 0000-0002-6716-1605

Handling Editor: David M. Tobin
Received 7 November 2021; Accepted 8 February 2022

Disease Models & Mechanisms (2022) 15, dmm049387. doi:10.1242/dmm.049387

expressed exclusively in cells of the macrophage lineage (Grabert et al., 2020) so the effect on hepatocytes must reflect indirect impacts of expansion of liver monocyte-macrophage populations. CSF1-Fc improved healing in paracetamol-induced acute liver failure in mice, increased regeneration of healthy liver following partial hepatectomy (PHx) (Stutchfield et al., 2015) and promoted recovery from ischaemia reperfusion injury in fibrotic liver (Konishi et al., 2020). These data suggest that CSF1 has therapeutic potential in liver disease. Infusion of CSF1-differentiated bone marrow-derived macrophages showed promise in murine models and is currently being tested in the clinic (Dwyer et al., 2021; Thomas et al., 2011). However, some of the earliest studies of CSF1 in disease models also showed the potential for exacerbation of inflammatory pathology (Hume and MacDonald, 2012), and macrophage depletion with anti-CSF1R or anti-CSF1 was previously shown to ameliorate development of toxin-induced liver fibrosis in mice (Mehal et al., 2001; Seifert et al., 2015). Here, we tested the therapeutic potential of CSF1-Fc and the role of macrophages in resolution of liver fibrosis in a non-resolving model of chronic inflammatory liver injury.

RESULTS

Chronic CSF1-Fc treatment prevents progression of established fibrosis after cessation of injury

The model we used is chronic exposure to thioacetamide (TAA) in the drinking water. Both TAA and the more-widely employed carbon tetrachloride (CCl4) model induce a sustained sterile injury to hepatocytes (similar to alcohol, for example), leading to progressive inflammation and fibrogenesis. The CCl4 model has previously been used to investigate macrophage contributions to fibrosis progression and regression (Duffield et al., 2005; Ramachandran et al., 2012; Thomas et al., 2011) but, unlike TAA-induced injury, CCl4 hepatotoxicity and fibrosis rapidly and spontaneously resolves (Liu et al., 2020; Ramachandran et al., 2012).

Previous studies have shown that acute porcine (P)-CSF1-Fc treatment (four daily injections of 1 mg/kg) led to a monocytosis, monocyte-macrophage accumulation in liver, hepatocyte proliferation and liver growth (Gow et al., 2014; Irvine et al., 2020; Sauter et al., 2016). In a pilot experiment, mice treated twice weekly with 1 mg/kg P-CSF1-Fc commencing at the same time as TAA administration experienced rapid onset of toxicity and did not survive past day 10-14. The CSF1-Fc treatment greatly exacerbated the hepatic pericentral inflammatory infiltration that commences within 1 week of TAA exposure (Melino et al., 2016). This was associated with alpha smooth muscle actin (αSMA) expression but not collagen deposition, nor extensive hepatocyte necrosis (Fig. S1). These observations indicate that TAA does not prevent the response to CSF1-Fc and vice versa and, not surprisingly, increasing monocyte recruitment in a setting of ongoing acute injury associated with generation of damage-associated molecular patterns (DAMPs) promotes pathology.

To model treatment of established liver disease in humans following removal of the primary stimulus, we tested the impact of CSF1-Fc treatment on liver fibrosis resolution after TAA cessation. In addition to P-CSF1-Fc, these experiments used a human CSF1-mouse Fc conjugate (HM-CSF1-Fc), which was developed by Novartis for evaluation in preclinical models. HM-CSF1-Fc was used at 5 mg/kg as initial studies demonstrated this dose induced a comparable biological response to 1 mg/kg P-CSF1-Fc (Fig. S2; see Materials and Methods for further details of CSF1-Fc reagents). Female mice were administered TAA in drinking water for 8 weeks or provided normal drinking water, followed by TAA withdrawal and twice-weekly treatment with CSF1-Fc or saline for 4 weeks, with sacrifice 1 day following the final dose. Additional groups of mice were left to recover for a further 4 weeks (i.e. 8 weeks post TAA withdrawal; Fig. 1A). Blood monocyte count was no longer elevated in CSF1-Fc-treated mice by this time point (Fig. 1B), but liver monocyte and macrophage content was increased, reflected by increased mRNA expression of the monocyte chemokine *Ccl2* and receptor *Ccr2*, as well as *Adgre1* (encoding the monocyte/macrophage marker F4/80), particularly in TAA-treated mice (Fig. 1C-E). Flow cytometry analysis of disaggregated liver confirmed the increases in both monocyte-derived ($F4/80^{Hi}$/TIM4^{-}) and resident ($F4/80^{Hi}$/TIM4+) liver macrophages and the infiltration of monocytes ($F4/80^{Low}$/$Cd11b^{Hi}$) in CSF1-Fc-treated mice (Fig. S3A-C). CSF1 drives the maturation of $Ly6C^{Hi}$ into $Ly6C^{Low}$ monocytes, which have previously been associated with resolution of liver fibrosis (Ramachandran et al., 2012), and their subsequent differentiation into macrophages. Consistent with this, a higher proportion of liver macrophages in CSF1-Fc-treated livers were monocyte-derived (TIM4^{-}) compared with saline-treated mice (Fig. S3B). Together, these data demonstrate that CSF1-Fc promotes recruitment and maturation of monocytes in the liver regardless of previous injury in response to TAA exposure. The increase in hepatic monocyte/macrophages was reversible and had returned to baseline 4 weeks after the cessation of CSF1-Fc treatment (Fig. 1C-E).

CSF1-Fc treatment increased the size of both the liver and spleen in control mice as reported previously (Gow et al., 2014). This response was also observed in TAA-exposed mice and returned to baseline 4 weeks after cessation of treatment (Fig. 1F,G). CSF1-Fc-induced liver growth was associated with proliferation of non-parenchymal cells (Fig. 1H,I; Fig. S4A). Among liver mitogens, previous analysis has revealed that acute CSF1-Fc treatment induced expression of heparin-binding EGF-like growth factor (*Hbegf*) in healthy mice, but did not affect epidermal growth factor (*Egf*), hepatocyte growth factor (*Hgf*), transforming growth factor alpha (*Tgfa*) or amphiregulin (Gow et al., 2014). *Hgf* mRNA increased upon TAA cessation, but was not further induced by CSF1-Fc (Fig. 1J). Both CSF1-Fc reagents induced *Hbegf* regardless of liver injury, as well as transforming growth factor, beta 1 (*Tgfb1*), an established mediator of fibroblast activation and fibrosis that also drives the resident liver macrophage transcriptional programme (Sakai et al., 2019) (Fig. 1K,L).

Eight weeks of TAA administration induced bridging fibrosis/cirrhosis (Fig. 2A). Histological inflammation (not shown) and expression of the major fibrillar collagens *Col1A1* and *Col3A1* (Fig. 2B; Fig. S4B) was reduced 4 weeks after TAA cessation. Expression of *Acta2* (encoding αSMA), generally considered a marker of myofibroblast/stellate cell activation, was variable and was not significantly elevated by TAA or CSF1-Fc in this chronic model (Fig. 2C). Acute CSF1-Fc treatment was previously reported to induce hepatic expression of inflammatory cytokines including *Il6* and *Tnf* (Stutchfield et al., 2021 preprint). *Il6* was significantly upregulated by chronic CSF1-Fc treatment in healthy but not TAA-treated liver, whereas *Tnf* was upregulated during TAA regression and not further regulated by CSF1-Fc (Fig. S4C,D).

Consistent with previous reports in the TAA model (Delire et al., 2015; Popov et al., 2011), fibrosis did not spontaneously regress following removal of the stimulus. In fact there was a further small increase in fibrotic area 4 weeks after TAA cessation (Fig. 2D), which was prevented by CSF1-Fc treatment. CSF1-Fc treatment induced expression of matrix remodelling genes including *Mmp9*, *Mmp13* and *Plau* (encoding plasminogen activator, urokinase;

Disease Models & Mechanisms (2022) 15, dmm049387. doi:10.1242/dmm.049387

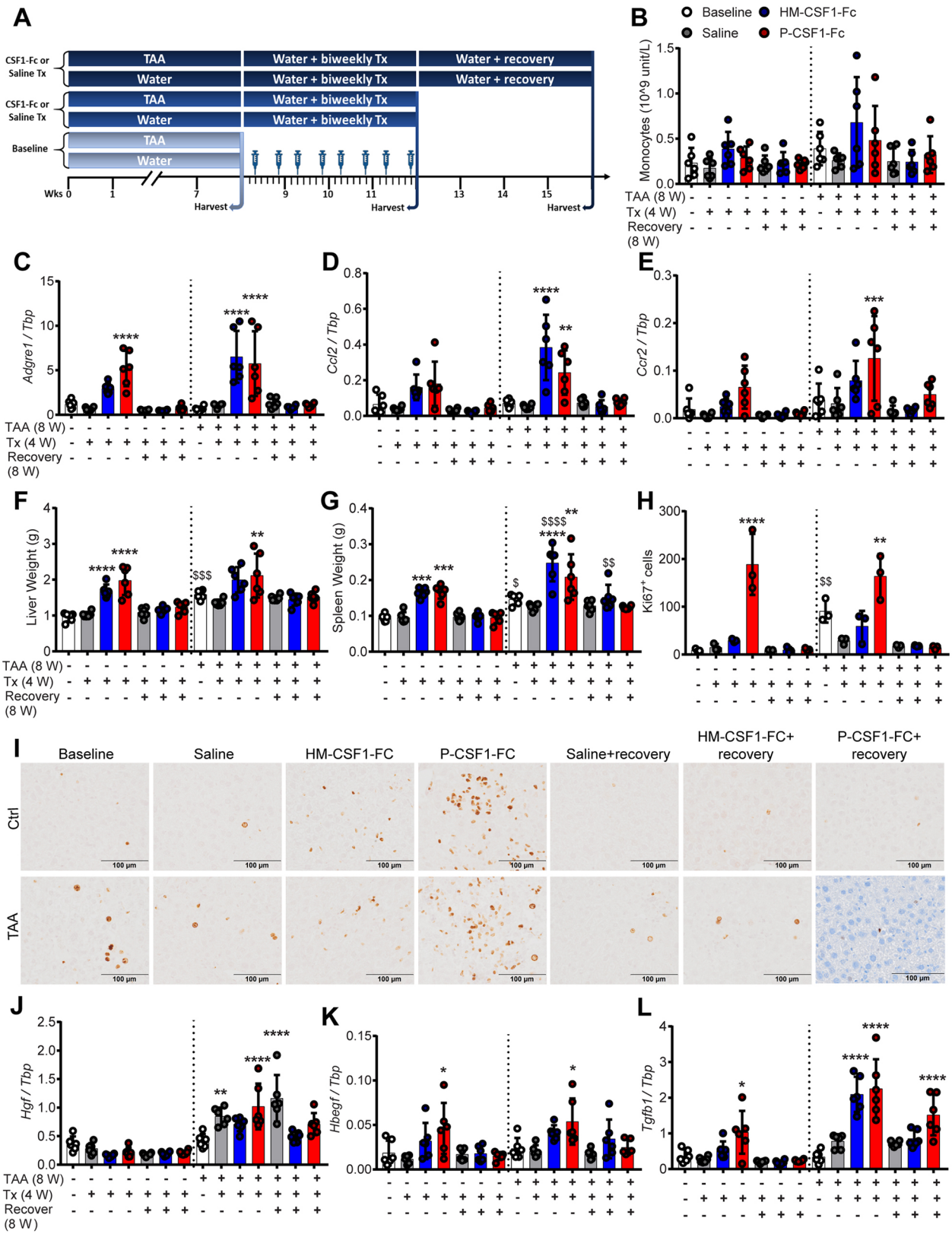

Fig. 1. Chronic CSF1-Fc-induced expansion of liver macrophages drives growth of chronically injured liver. (A) Groups of male mice were administered TAA or normal drinking water for 8 weeks (baseline), followed by cessation of TAA treatment and bi-weekly treatment with P-CSF-Fc, HM-CSF1-Fc or saline for 4 weeks [Tx (4 W)] or a further 4 weeks post-treatment recovery [Recovery (8 W)]. (B) Blood monocyte count. (C-E) Whole-liver expression of *Adgre1* (C), *Ccl2* (D) and *Ccr2* (E). (F,G) Liver (F) and spleen (G) weight. (H,I) Quantification (H) and representative immunohistochemistry images (I) of liver Ki67+ cells. (J-L) Whole-liver expression of *Hgf* (J), *Hbegf* (K) and *Tgfb1* (L). Data are mean±s.d. One-way ANOVA with multiple comparisons: **P*<0.05, ***P*<0.01, ****P*<0.001, *****P*<0.0001 comparing with baseline in the same group; $^{\$}$*P*<0.05, $^{\$\$}$*P*<0.01, $^{\$\$\$}$*P*<0.001, $^{\$\$\$\$}$*P*<0.0001 comparing the same treatment between groups (*n*=6 per group, with three animals per group randomly selected for immunohistochemistry image analysis).

Disease Models & Mechanisms (2022) 15, dmm049387. doi:10.1242/dmm.049387

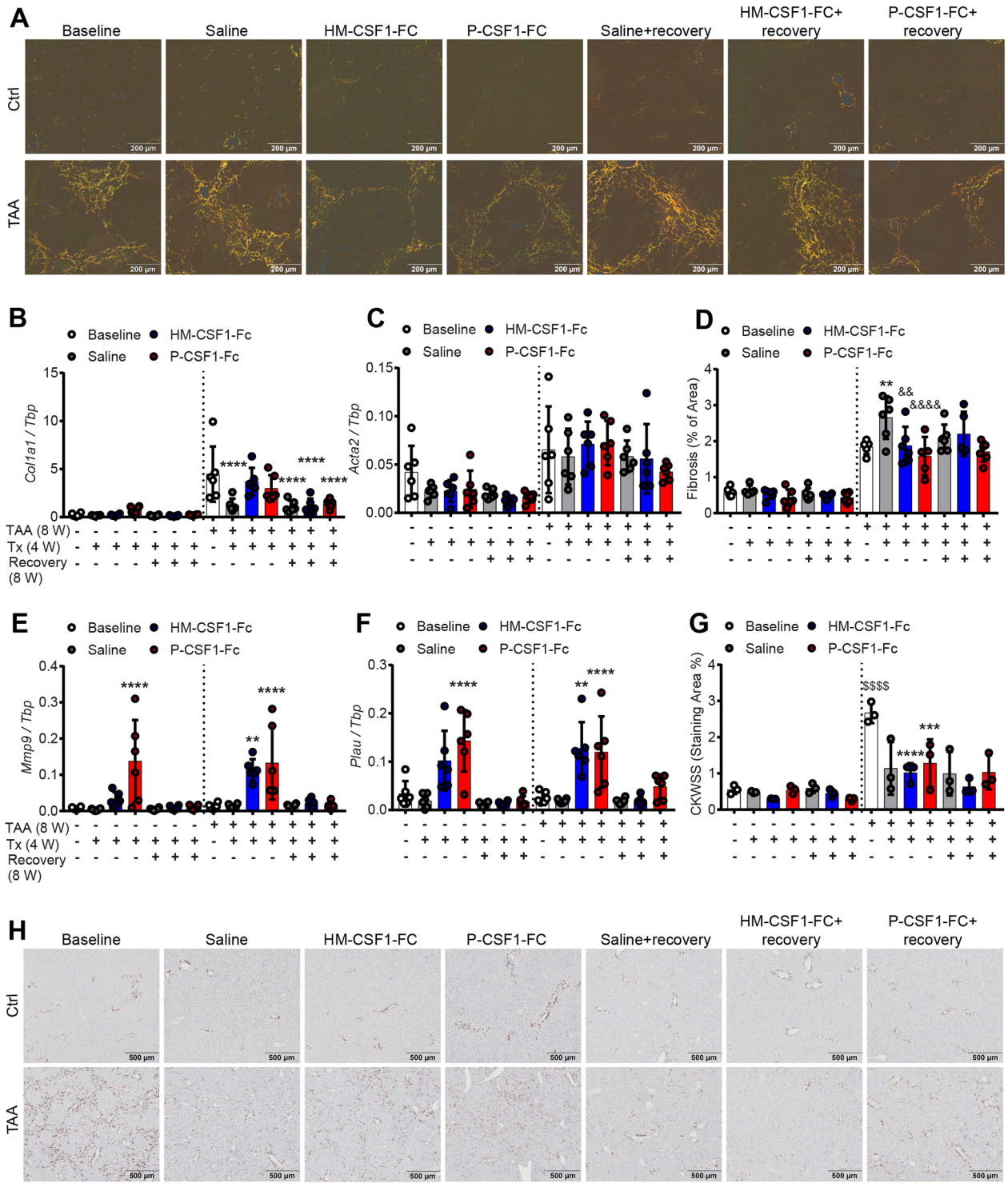

Fig. 2. Chronic CSF1-Fc treatment initiates resolution of established fibrosis. (A,D) Collagen was assessed by Picrosirius Red staining visualised under polarised light (A) and quantified by image analysis (D). (B,C,E,F) Expression of *Col1a1* (B), *Acta2* (C), *Mmp9* (E) and *Plau* (F) in whole liver was quantified by RT-PCR. (G,H) Quantification by image analysis (G) and hepatic progenitor cell activation, assessed by CKWSS immunohistochemistry (H). Experimental design as in Fig. 1A. Data are mean±s.d. One-way ANOVA with multiple comparison: $^{**}P<0.01$, $^{***}P<0.001$, $^{****}P<0.0001$ comparing with baseline in the same group; $^{\&\&}P<0.01$, $^{\&\&\&\&}P<0.0001$ comparing with saline in same group; $^{\$\$\$\$}P<0.0001$ comparing the same treatment between groups (n=6 per group with three animals per group randomly selected for immunohistochemistry image analysis).

uPA) (Fig. 2E,F; Fig. S4E). *Mmp9* is highly expressed by resident and recruited monocyte-derived macrophages in multiple mouse organs including liver (Summers et al., 2020). *Plau* is a CSF1R target gene in macrophages (Stacey et al., 1995). As in all chronic liver injury models, TAA induced prominent hepatic progenitor cell (HPC) activation, identified by wide-spectrum keratin (CKWSS) staining (Melino et al., 2016). Unlike the fibrosis, HPC activation largely resolved spontaneously by 4 weeks after TAA cessation in

Disease Models & Mechanisms (2022) 15, dmm049387. doi:10.1242/dmm.049387

saline-treated mice, and CSF1-Fc treatment had minimal impact (Fig. 2G,H), suggesting that HPC do not mediate CSF1-Fc-induced liver regeneration in TAA-treated mice.

To determine whether a less frequent CSF1-Fc treatment regime would effectively remodel the fibrotic scar, we investigated the impact of once weekly treatment on fibrosis regression. This regimen was effective in a fracture healing model (Batoon et al., 2021). Female mice were administered TAA for 8 weeks, followed by treatment with CSF1-Fc for up to 8 weeks (mice were sacrificed 1 week following the final dose). Weekly CSF1-Fc treatment did not significantly ameliorate fibrosis or persistently increase liver weight and the impact on macrophage and matrix remodelling gene expression at the 4 week time point was not sustained (Fig. S5A-E). This led us to question whether CSF1-Fc from other species induces an anti-drug antibody response that may limit the impact of treatment over time. Indeed, there was a significant anti-CSF1-Fc response in mice treated with either CSF1-Fc reagent (Fig. S5F,G). In overview, these studies indicate that CSF1-Fc treatment has the potential to initiate liver fibrosis resolution, but evaluation of chronic treatment regimens with existing reagents in mice is compromised by an anti-drug response.

Acute CSF1-Fc treatment is sufficient to eliminate established fibrosis

Previous studies of CSF1-Fc treatment in acute liver injury models used four successive daily injections (Stutchfield et al., 2015). To test an acute regime, male and female mice were treated with TAA for 8 weeks, followed by four daily injections of CSF1-Fc or saline before sacrifice on day 5 or before recovery on day 14 (Fig. 3A). This acute regime induced monocytosis and increased liver and spleen weight as expected (Fig. 3B-D). Here, we showed that this impact is rapidly reversible and had resolved by day 14. Acute CSF1-Fc induced *Adgre1*, *Ccl2* and *Ccr2* mRNA in the liver, consistent with an increase in monocytes and macrophages (Fig. 3E-G). As in the chronic treatment, CSF1-Fc transiently induced *Tgfb1*, but not *Il6* and *Tnf* (Fig. 3H-J). CSF1-Fc-induced liver growth was associated with an increase in Ki67+ parenchymal and non-parenchymal cells, which normalised by day 14 (Fig. 3K-M). No differences in *Hgf* or *Hbegf* expression were observed (Fig. 3N,O). CSF1-Fc did not increase CKWSS staining area, suggesting that HPC do not contribute to the large increase in proliferating non-parenchymal cells or to liver growth (Fig. 4A,B).

Acute CSF1-Fc treatment promoted a significant reduction in fibrotic area, especially in the females, which were more severely affected (Fig. 4C,D). This effect was partly reversed by day 14 post treatment. Fibrosis regression was associated with transient increases in *Mmp9* and *Plau* expression on day 5, which also returned to baseline by day 14 (Fig. 4G,H). Surprisingly, CSF1-Fc treatment also produced a significant transient increase in *Acta2* mRNA encoding αSMA and *Col1a1* in female mice (Fig. 4E,F). In saline-treated mice, αSMA was restricted to sinusoidal myofibroblasts. By contrast, in CSF1-Fc-treated mice increased αSMA expression co-localised with F4/80+ macrophages (Fig. 4I,J).

CSF1-Fc treatment reduces fibrosis and improves fibrotic liver regeneration after PHx

Liver regenerative capacity in patients with advanced fibrosis is compromised, which limits surgical intervention (Hackl et al., 2016; Krenzien et al., 2018). To model application of acute CSF1-Fc treatment in this indication, we established fibrosis using 8 weeks of TAA treatment, then performed a 50% PHx. Mice were treated with CSF1-Fc or saline for 2 days before and 2 days after surgery, followed by sacrifice on day 3 (Fig. 5A). Mice with both healthy and fibrotic liver treated with CSF1-Fc gained weight post-surgery more rapidly and had increased liver and spleen mass on day 3 (Fig. 5B-D). CSF1-Fc treatment increased circulating monocytes, as well as liver *Adgre1*, *Ccl2* and *Ccr2* expression (Fig. 5E-H). PHx-induced liver regrowth was associated with an increase in proliferative (Ki67+) hepatocytes and non-parenchymal cells in the remnant liver, which was partly compromised in fibrotic livers (Fig. 5J-L). CSF1-Fc treatment increased Ki67+ non-parenchymal cells but did not further increase Ki67+ hepatocytes at this time point, and did not overcome the deficit in the fibrotic livers (Fig. 5K,L). Nevertheless, CSF1-Fc-treated mice had substantial increases in mRNA encoding *Hbegf*, *Tgfb1*, *Il6* and *Tnf* (Fig. 5O-R), each of which could contribute to hepatic growth (Kiso et al., 2003; Michalopoulos and Bhushan, 2021). *Hgf* and *Brg1* (also known as *Smarca4*), a chromatin remodelling gene involved in liver regeneration (Wang et al., 2019), were more highly expressed following PHx in fibrotic liver compared with healthy liver (Fig. 5I,S). Neither PHx nor CSF1-Fc affected HPC abundance (Fig. 5J,N). CSF1-Fc treatment almost completely eliminated fibrosis in this model (Fig. 5J,M). This was associated with reduced hepatic *Col3a1* but not *Col1a1* expression (Fig. 6A,B). The CSF1-Fc-induced fibrosis resolution was again associated with increases in *Mmp9* and *Plau* (Fig. 6C,D).

One consequence of CSF1 treatment in animals and humans (Baker and Levin, 1998; Garnick and O'Reilly, 1989) is a reversible reduction in blood platelets. We observed an extended clotting time, lower platelet count (Fig. 6E), reduced serum albumin (Fig. 6F) and apparent ascites in CSF1-Fc-treated mice that had undergone PHx. Serum liver enzymes (ALT and AST) did not indicate increased hepatocellular injury; indeed ALP was significantly reduced by CSF1-Fc treatment, and there was no change in bile acids (Fig. 6G-J). Nevertheless, thrombocytopaenia is of concern in CLD patients, especially those undergoing surgery.

To determine whether these impacts of CSF1-Fc could be avoided, while retaining desirable impacts on liver regeneration and fibrosis, we tested the efficacy of a sub-maximal dose of CSF1-Fc ('low-dose'). Male mice were administered TAA or normal drinking water for 12 weeks, treated with 1 mg/kg HM-CSF1-Fc or saline control for 2 days before and 2 days after 50% Phx, and sacrificed 3 or 7 days post-surgery (Fig. 7A). Half of the mice in the 7-day recovery group were randomly assigned to undergo blood flow imaging on day 3 post-surgery. Although low-dose CSF1-Fc did not induce monocytosis in healthy mice (Fig. S2B) it did increase blood monocytes in TAA-exposed animals on day 3 post-surgery, which largely normalised by day 7 (Fig. 7B). Low dose CSF1-Fc treatment still accelerated body and liver weight gain post-surgery, increased spleen weight (Fig. 7C-E) and transiently induced hepatic *Adgre1*, *Ccl2* and *Ccr2* expression (Fig. 7F-H). Low dose CSF1-Fc induced *Hbegf* and *Tgfb1*, but not *Hgf*, on day 3 post surgery (Fig. 7I-K) and greatly increased the number of Ki67+ proliferating non-parenchymal cells on day 3 (Fig. 7L-O). Low-dose CSF1-Fc still promoted resolution of hepatic fibrosis by day 3, which persisted to day 7 (Fig. 7P,Q). The treatment did not impact *Col1a1* expression but induced sustained *Mmp9* elevation in both healthy and fibrotic liver, and transient induction of *Plau* (Fig. 8A-C). The low dose did not completely prevent the thrombocytopaenia or reduced circulating albumin, but no ascites or clotting impairment were evident and these parameters were fully resolved by day 7 (Fig. 8D,E). Serum ALT and ALP were reduced in CSF1-Fc-treated mice (Fig. 8F,G). Doppler imaging showed decreased liver

Disease Models & Mechanisms (2022) 15, dmm049387. doi:10.1242/dmm.049387

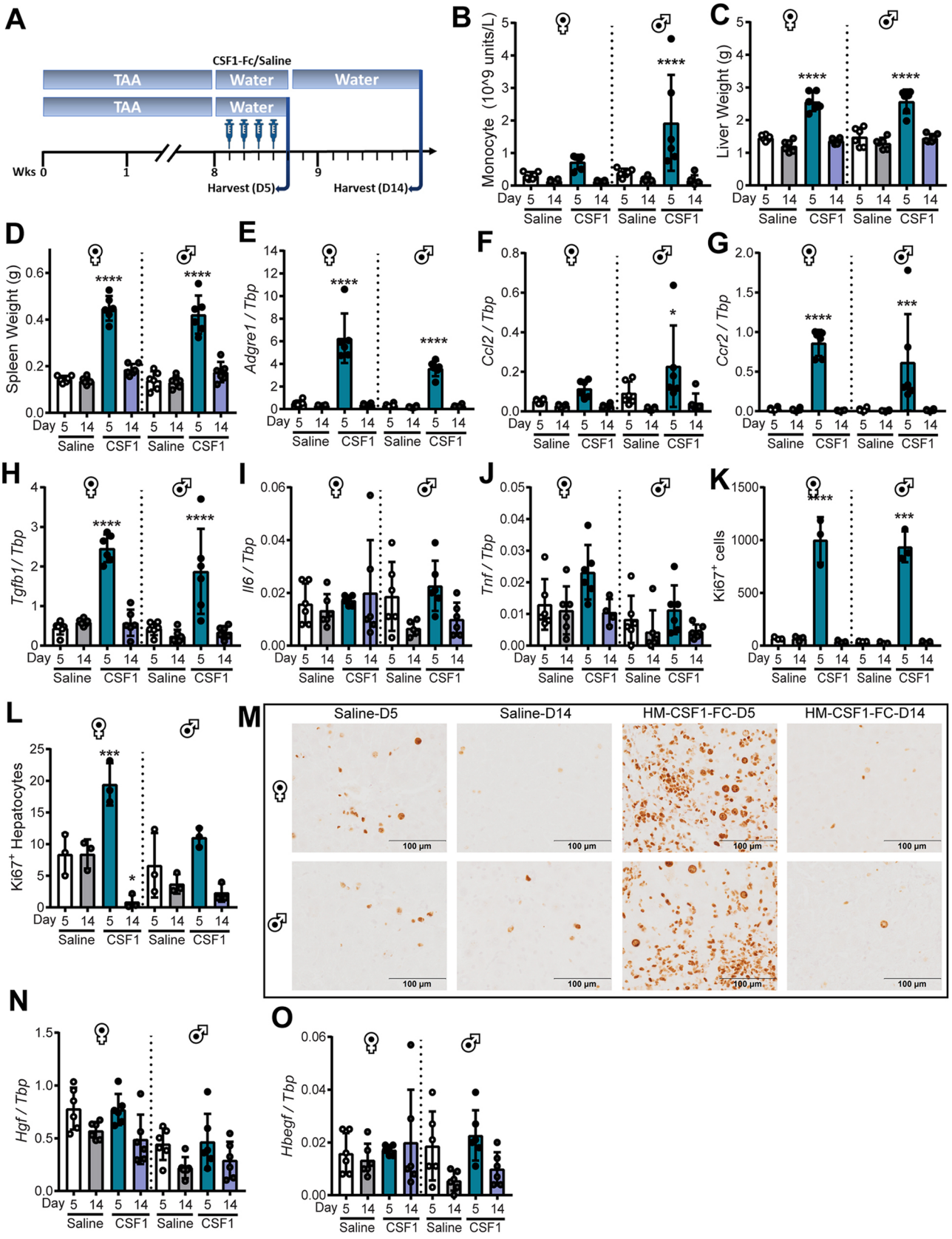

Fig. 3. Acute CSF1-Fc-induced expansion of liver macrophages drives growth of chronically injured liver. (A) Male and female mice were administered TAA for 8 weeks, before daily treatment with HM-CSF1-Fc or saline for 4 days and sacrificed on day 5 or day 14. (B) Blood monocyte count. (C) Liver weight. (D) Spleen weight. (E-J,N,O) Whole-liver expression of *Adgre1* (E), *Ccl2* (F), *Ccr2* (G), *Tgfb1* (H), *Il6* (I), *Tnf* (J), *Hgf* (N) and *Hbegf* (O). (K,L) Liver Ki67+ cells (K) and hepatocytes (L). (M) Representative immunohistochemistry images of liver Ki67+ cells. Data are mean±s.d. One-way ANOVA with multiple comparison: **P*<0.05, ****P*<0.001, *****P*<0.0001 comparing with saline day 5 in the same group (*n*=6 per group, with three animals per group randomly selected for immunohistochemistry image analysis).

Disease Models & Mechanisms (2022) 15, dmm049387. doi:10.1242/dmm.049387

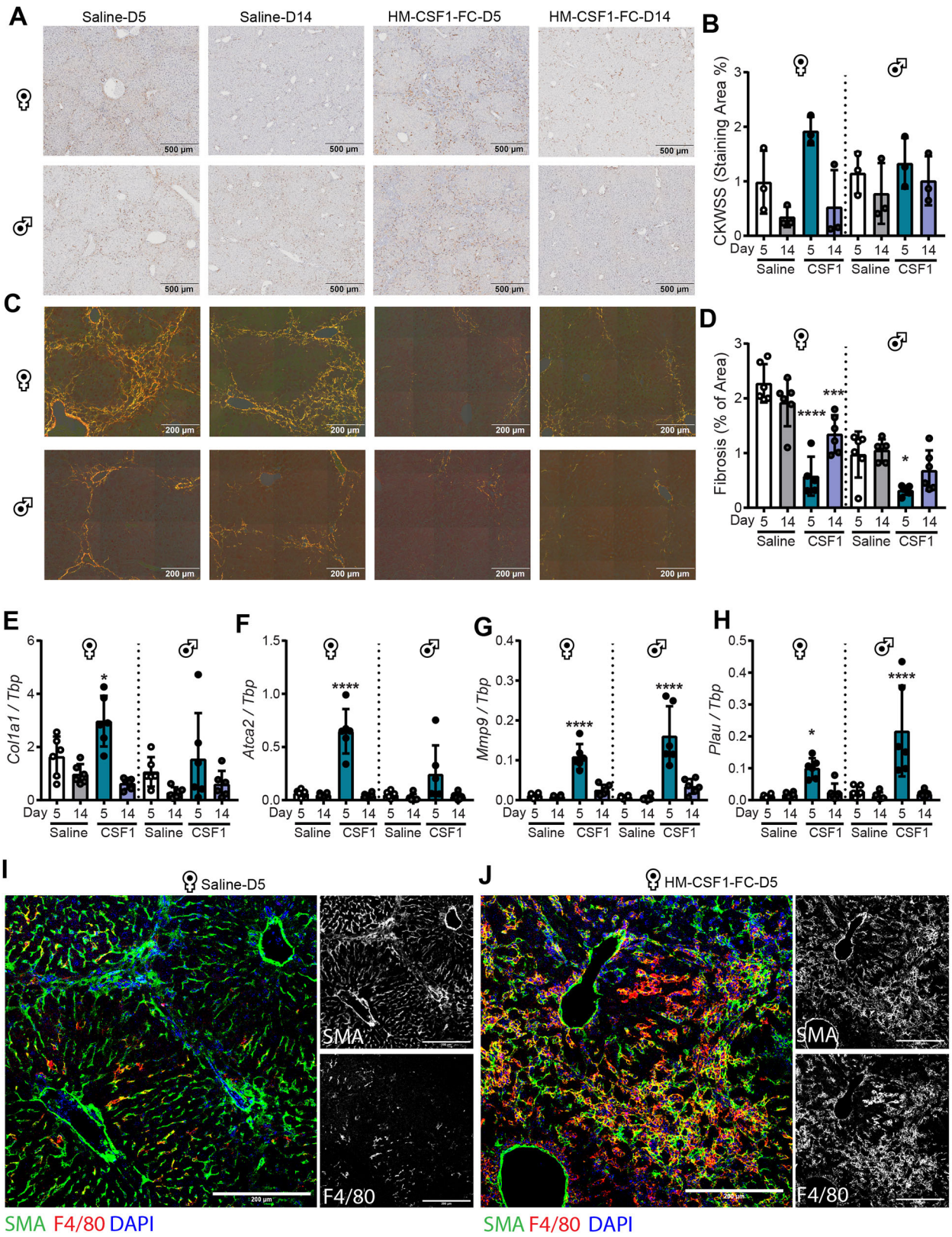

Fig. 4. Acute CSF1-Fc treatment resolves established fibrosis. (A,B) Hepatic progenitor cell activation was visualised by CKWSS immunohistochemistry (A) and quantified (B). (C,D) Collagen was assessed by Picrosirius Red staining visualised under polarised light (C) and quantified (D). (E-H) Whole-liver expression of *Col1a1* (E), *Acta2* (F), *Mmp9* (G) and *Plau* (H). (I,J) Representative SMA and F4/80 staining in saline (I) and CSF1-Fc (J)-treated liver (one representative animal per group). Experimental design as in Fig. 3A. Data are mean±s.d. One-way ANOVA with multiple comparison: **P*<0.05, ****P*<0.001, *****P*<0.0001 comparing with saline day 5 in the same group (*n*=6 per group, with three animals per group randomly selected for immunohistochemistry image analysis).

Disease Models & Mechanisms (2022) 15, dmm049387. doi:10.1242/dmm.049387

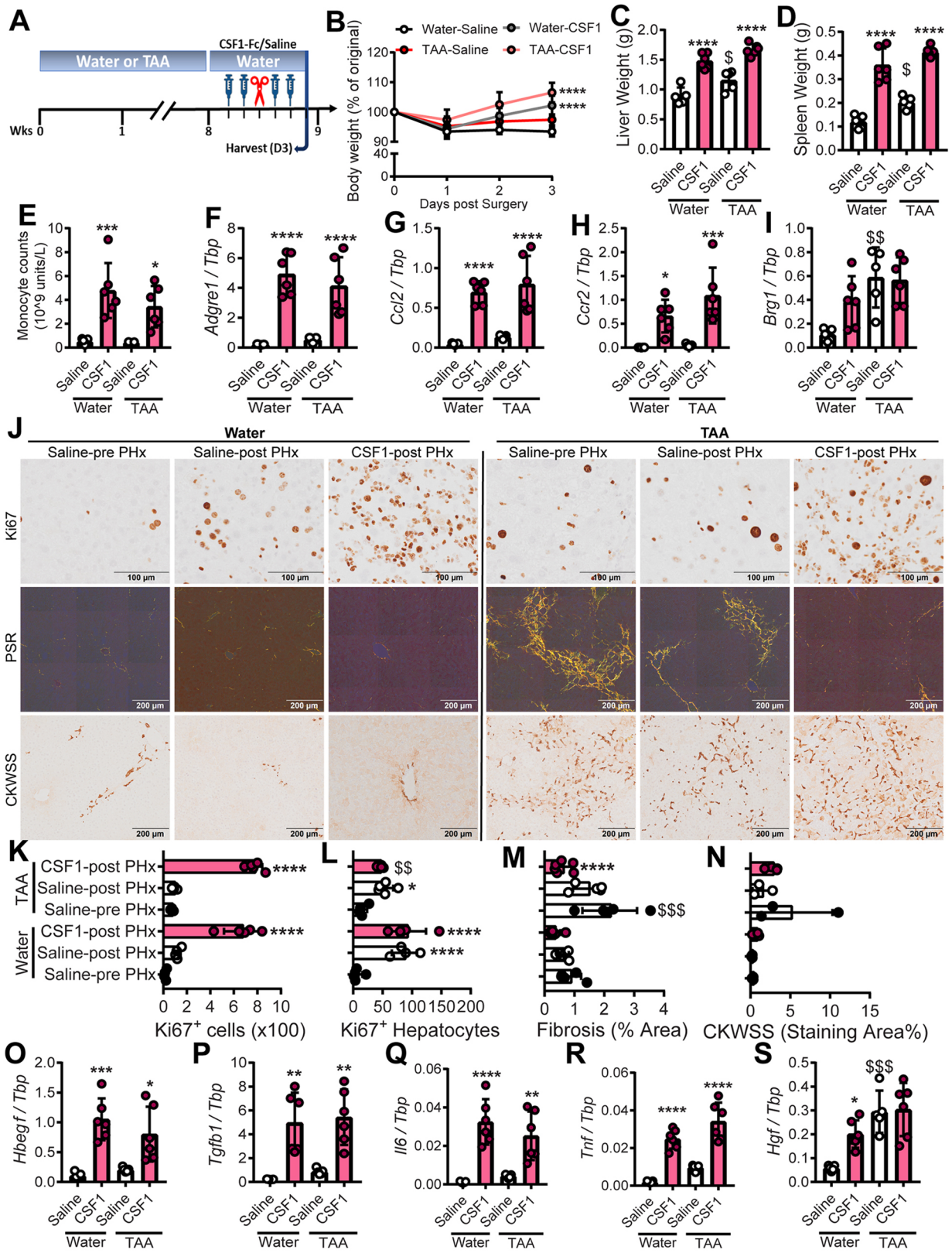

Fig. 5. CSF1-Fc promotes liver regrowth and fibrosis resolution post-resection. (A) Male mice were administered TAA or normal water for 8 weeks, treated with P-CSF1-Fc or saline pre- and post-50% hepatectomy and then sacrificed on day 3. (B) Body weight. (C) Liver weight. (D) Spleen weight. (E) Blood monocytes. (F-I,O-S) Whole-liver expression of *Adgre1* (F), *Ccl2* (G), *Ccr2* (H), *Brg1* (I), *Hbegf* (O), *Tgfb1* (P), *Il6* (Q), *Tnf* (R) and *Hgf* (S). (J,K,L) Representative images (J) and quantification (K,L) of Ki67+ cells. Collagen (Picrosirius Red; J,M). HPC (CKWSS; J,N). Data are mean±s.d. One-way ANOVA with multiple comparison: **P*<0.05, ***P*<0.01, ****P*<0.001, *****P*<0.0001 comparing with saline in the same group; $^{\$}$*P*<0.05, $^{\$\$}$*P*<0.01, $^{\$\$\$}$*P*<0.001 comparing the same treatment between groups (*n*=3 per group for water treatment and 6 per group for TAA treatment, with three animals per group randomly selected for immunohistochemistry image analysis).

Disease Models & Mechanisms (2022) 15, dmm049387. doi:10.1242/dmm.049387

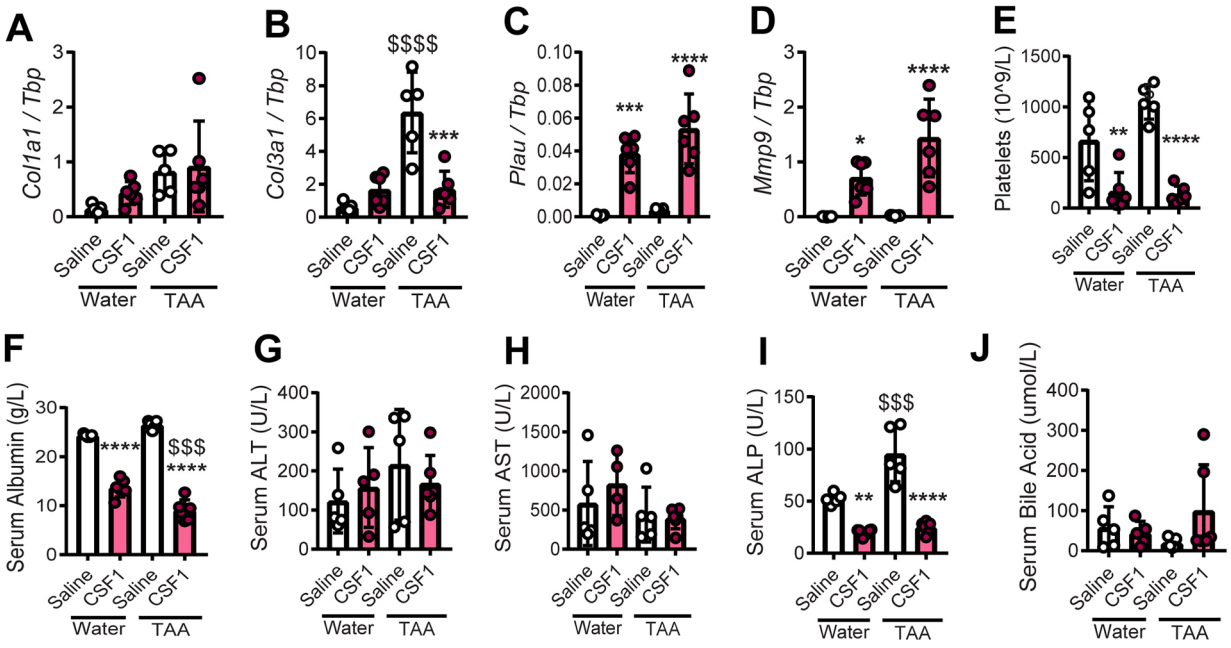

Fig. 6. Impacts of acute CSF1-Fc treatment on hepatic gene expression and serum biochemistry post-resection. (A-D) Whole-liver expression of *Col1a1* (A), *Col3a1* (B), *Plau* (C) and *Mmp9* (D). (E-J) Quantification of circulating platelets (E), serum albumin (F), ALT (G), AST (H), ALP (I) and bile acids (J). Experimental design as in Fig. 5A. Data are mean±s.d. One-way ANOVA with multiple comparison: **P*<0.05, ***P*<0.01, ****P*<0.001, *****P*<0.0001 comparing with saline in the same group; $^{\$\$\$}$*P*<0.001, $^{\$\$\$\$}$*P*<0.0001 comparing the same treatment between groups (*n*=3 per group for water treatment and 6 per group for TAA treatment).

vascularisation in TAA-treated mice compared with healthy mice on day 3 post-PHx, which was reversed by low-dose CSF1-Fc treatment (Fig. 8H,I).

DISCUSSION

Resolution of fibrosis and liver regeneration after surgical resection are unmet clinical needs. CSF1 and CSF1R are potential targets of anti-inflammatory treatments being developed by several pharmaceutical companies (Denny and Flanagan, 2021; Hamilton et al., 2016). CSF1 is a homeostatic growth factor that supports the trophic and matrix remodelling functions of macrophages during development and adult tissue maintenance, and which has been shown to promote liver growth in healthy mammals (Gow et al., 2014; Irvine et al., 2020; Sauter et al., 2016). Here, we demonstrated that CSF1-Fc can promote hepatocyte proliferation and liver growth in chronically diseased liver, including after surgery. We also demonstrated that acute and chronic CSF1-Fc treatment significantly reduced the extensive fibrosis caused by long-term exposure to TAA, which does not resolve spontaneously, and even continued to increase after TAA withdrawal. This is similar to alcoholic hepatitis, which continues to progress in many patients after alcohol cessation (Artru et al., 2017; Hosseini et al., 2019). The underlying mechanisms are not well understood, but the interpretation is that the inflammatory process becomes self-sustaining in the absence of injury, likely due in part to depletion of hepatocyte anti-oxidant defences and damage to cellular components caused by reactive metabolites (Balkan et al., 2001). The striking reduction in fibrosis in response to acute CSF1-Fc treatment was partially reversed by day 14, paralleling the transient expansion in monocytes/macrophages, which is regulated by growth factor availability (Bartocci et al., 1987). There is potential to investigate and optimise the chronic treatment regimes used here (Figs 1, 2; Fig. S5), in which efficacy was likely compromised by the anti-drug antibody response, to achieve lasting resolution of fibrosis. We are currently developing a fully-orthologous mouse CSF1-Fc protein.

The therapeutic response to CSF1-Fc was associated with increased liver macrophages, a relative preponderance of the Ly6C^{Low} monocyte phenotype; and increased expression of matrix remodelling factors *Mmp9* and *Plau*. MMP9 overexpression promoted a pro-resolving macrophage phenotype and improved liver regeneration in cirrhotic mice (Melgar-Lesmes et al., 2018). uPA (*Plau*) therapy ameliorated fibrosis in the CCl4 model via activation of latent metalloproteinases and HGF (Bueno et al., 2006; Meza-Rios et al., 2016; Salgado et al., 2000). Fibrosis regression occurred despite high expression of the canonical pro-fibrogenic cytokine *Tgfb1* and, in some cases, the pro-inflammatory cytokines *Il6* and *Tnf*, which have frequently been shown to diminish in the resolution phase of disease. Given its pivotal role in the transcriptional programme driving liver macrophage differentiation (Sakai et al., 2019), it is possible that *Tgfb1* is directly or indirectly induced by CSF1. Indeed, it is highly-expressed by mouse bone marrow-derived and thioglycolate-elicited macrophages (Biogps.org). The unexpected macrophage αSMA expression in response to CSF1-Fc treatment may indicate TGFβ signalling in macrophages. αSMA+ macrophages were described previously in a foreign body response (Mooney et al., 2010), and αSMA-expressing macrophages have also been implicated in protecting the bone marrow environment from radiation-induced injury (Ludin et al., 2012). Hence, in the context of tissue injury, αSMA+ cannot be considered a myofibroblast marker. It is also possible that *Tgfb1* is induced as a response to rapid liver growth to limit expansion, given its known anti-proliferative function (Michalopoulos and Bhushan, 2021).

In healthy mice, CSF1-Fc-induced liver growth was associated with an increase in Ki67+ hepatocytes as well as non-parenchymal cells, whereas the large increase in hepatic Ki67+ cells in TAA-treated mice was largely in the non-parenchymal compartment,

Disease Models & Mechanisms (2022) 15, dmm049387. doi:10.1242/dmm.049387

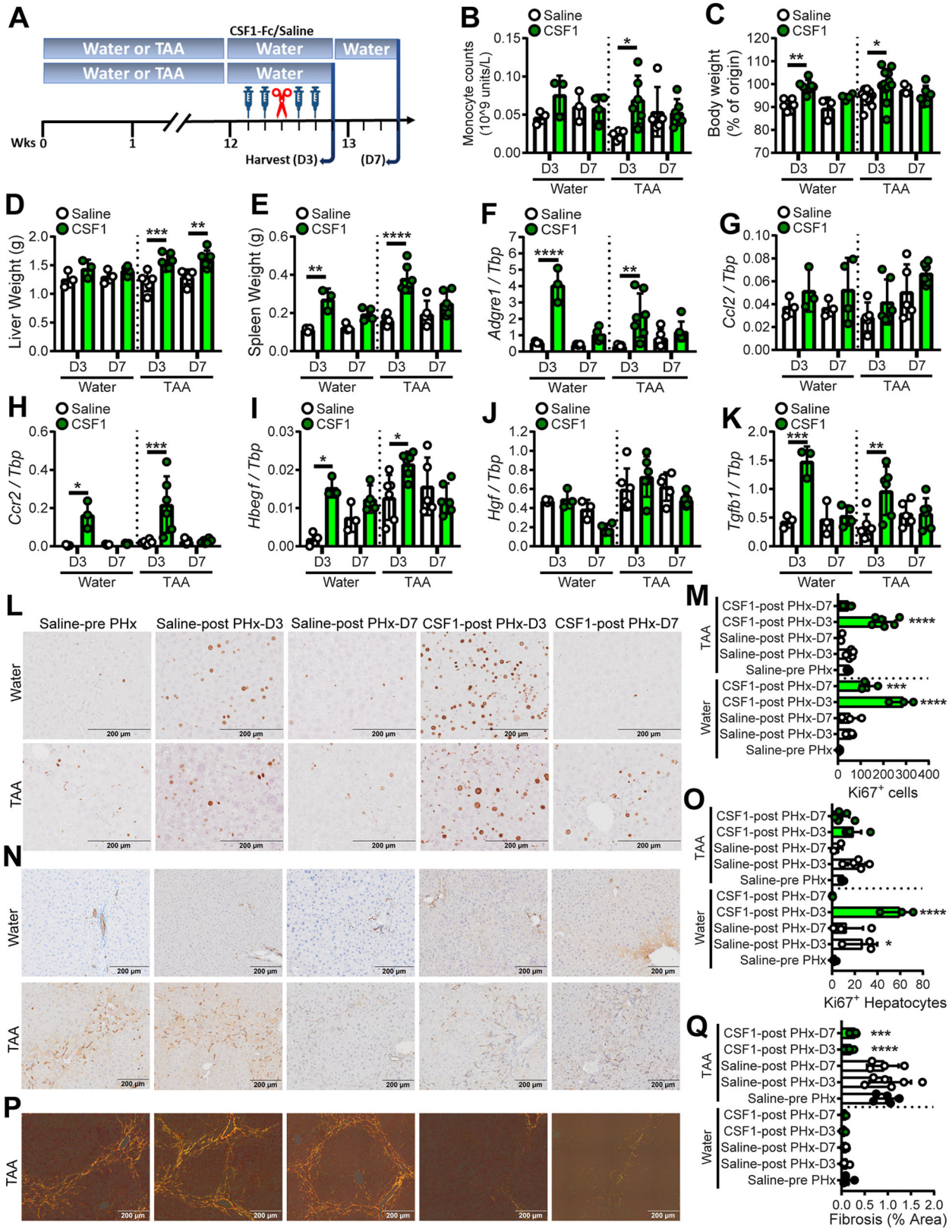

Fig. 7. Low-dose CSF1-Fc treatment promotes liver regrowth and fibrosis resolution post-resection. (A) Male mice were administered TAA or normal water for 12 weeks, then treated with HM-CSF1-Fc or saline pre- and post-50% hepatectomy and sacrificed on day 3 or 7. (B) Blood monocyte count. (C) Body weight. (D) Liver weight. (E) Spleen weight. (F-K) Whole-liver expression of *Adgre1* (F), *Ccl2* (G), *Ccr2* (H), *Hbegf* (I), *Hgf* (J) and *Tgfb1* (K). (L,M) Representative images (L; Ki67 staining) and quantification (M) of liver Ki67+ cells. (N,O) Representative images (N; CKWSS) and quantification (O) of liver HPC. (P,Q) Representative images (P; Picrosirius Red) and quantification (Q) of liver collagen. Data are mean±s.d. One-way ANOVA with multiple comparison: **P*<0.05, ***P*<0.01, ****P*<0.001, *****P*<0.0001 comparing with saline pre-PHx in the same group (*n*=3 per group for water treatment and 6 per group for TAA treatment, with three animals per group randomly selected for immunohistochemistry image analysis).

Disease Models & Mechanisms (2022) 15, dmm049387. doi:10.1242/dmm.049387

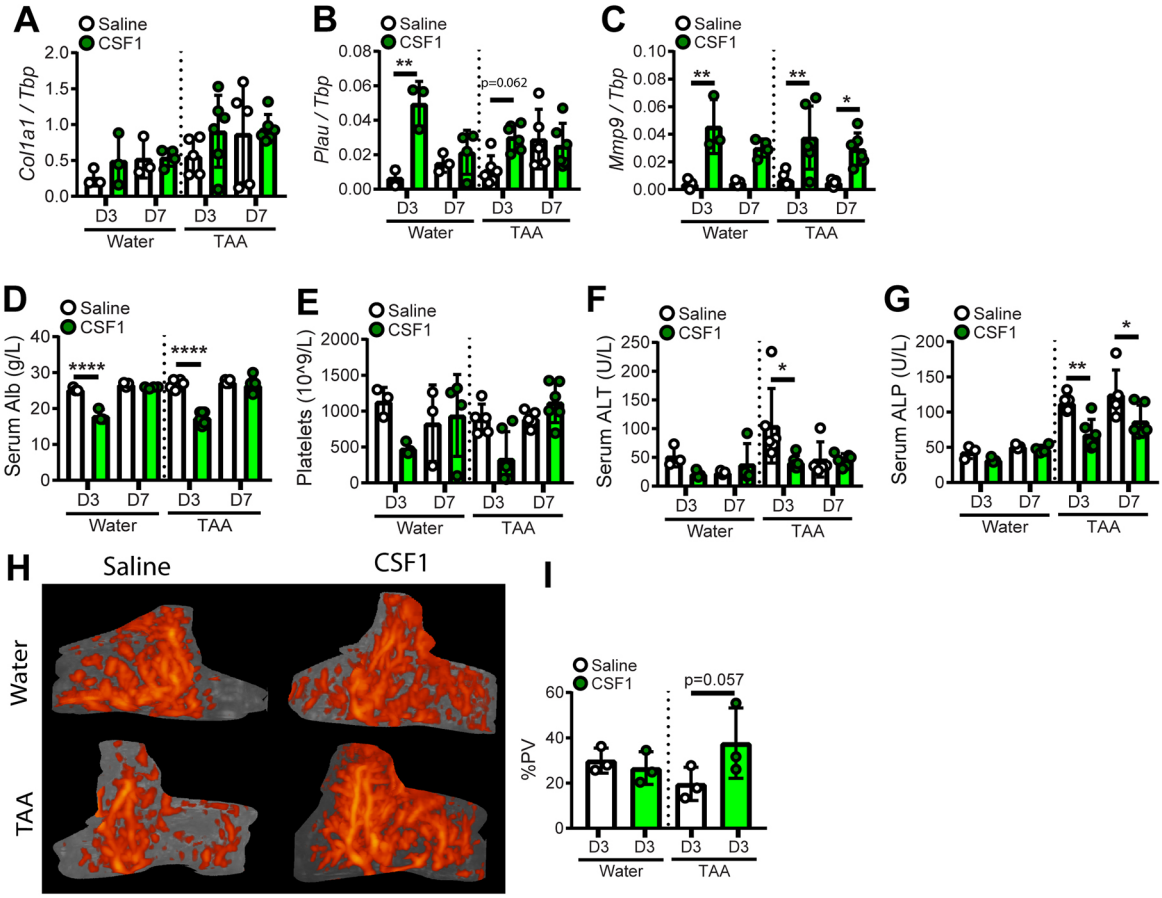

Fig. 8. Impacts of low-dose CSF1-Fc treatment on hepatic gene expression, serum biochemistry and hepatic blood flow post-resection. (A-C) Whole-liver expression of *Col1a1* (A), *Plau* (B) and *Mmp9* (C). (D-G) Serum albumin (D), circulating platelets (E), serum ALT (F) and ALP (G). (H,I) Hepatic blood flow was assessed by Power Doppler imaging (H) and quantified (I). Experimental design as in Fig. 7A. Data are mean±s.d. One-way ANOVA with multiple comparison: **P*<0.05, ***P*<0.01, *****P*<0.0001 (*n*=3 per group for water treatment and 6 per group for TAA treatment, with three animals randomly selected for Doppler imaging).

consistent with evidence of impaired hepatocyte-mediated regeneration in chronically injured liver (Holczbauer et al., 2021). We hypothesised this may reflect a role for HPC. The function of HPC activation and the ductular reaction in liver fibrogenesis versus regeneration is controversial (Michalopoulos and Bhushan, 2021; So et al., 2020; Williams et al., 2014). PHx in fibrotic liver was previously reported to drive pro-fibrogenic HPC activation that impaired liver regeneration (Kuramitsu et al., 2013). On the other hand, adoptive transfer of CSF1-stimulated macrophages (BMDM) that reduced fibrosis in the CCl4 model was associated with TWEAK-dependent HPC activation (Thomas et al., 2011), and even transfer of BMDM into healthy mice induced transient macrophage TWEAK-dependent HPC activation (Bird et al., 2013). In the TAA model, HPC activation resolved spontaneously whereas fibrosis did not, and CSF1-Fc treatment had no effect in either healthy or TAA-exposed mice. Hence, we do not provide support for direct engagement of recruited macrophages with HPC in this setting. Alternative mechanisms that may contribute to liver growth, especially in fibrotic liver, may include hepatocyte hypertrophy, reductive cell division and immature hepatocytes (distinct from the ductular reaction) (Holczbauer et al., 2021; Miyaoka et al., 2012; Nakano et al., 2017).

Although our results are promising, some impacts of CSF1-Fc treatment could produce a dose-limiting toxicity in CLD patients and would need to be monitored. Splenomegaly and thrombocytopaenia occur in advanced liver disease and are associated with poor outcomes. Splenectomy improves liver function in patients with advanced liver disease, and also reduces fibrosis and augments liver function in mouse models (Yada et al., 2015; Zheng et al., 2020). Mechanistically, the spleen could be a source of circulating TGFB1 and the monocyte chemokine CCL2 (Li et al., 2018). Thrombocytopaenia in CLD is multi-factorial, including platelet sequestration, reduced production and increased destruction (Mitchell et al., 2016). Transient thrombocytopaenia was the dose-limiting toxicity in initial human clinical trials of CSF1 (Garnick and O'Reilly, 1989). This was further investigated in mice and found to be independent of the spleen and platelet production, and to resolve with prolonged treatment (Baker and Levin, 1998). The impact of CSF1 on platelets was rather attributed to increased activity of monocytes/macrophages, which shortened platelet survival. Platelet production was subsequently increased, which compensated for ongoing destruction (Baker and Levin, 1998). In the current study, we observed transient thrombocytopaenia, even with low-dose CSF1-Fc, but this was rapidly resolved. We also observed a transient reduction in circulating albumin, but no evidence of liver injury. Overall, CSF1 was well-tolerated in human clinical trials, even with two consecutive continuous 7 day infusions (Jakubowski et al., 1996), and CSF1-Fc has also been tested in pigs (Sauter et al., 2016).

In conclusion, strategies to 'reprogramme' macrophages have significant therapeutic potential via stimulation of multiple

Disease Models & Mechanisms (2022) 15, dmm049387. doi:10.1242/dmm.049387

coordinated pro-regenerative macrophage functions, including phagocytosis, matrix remodelling, angiogenesis and production of tissue trophic factors. Here, we have demonstrated striking impacts of CSF1-Fc on fibrosis and regrowth of fibrotic liver post-PHx. The therapeutic impacts may be attributable to CSF1 signalling specifically and/or driven by the increase in liver macrophages and amplified within the tissue microenvironment. The timing of intervention is crucial because macrophages are shaped by the evolving microenvironment at the site of injury, as clearly illustrated by the different outcomes of CSF1-Fc treatment during and after cessation of liver injury. Further delineation of the molecular programmes that drive restorative macrophage activities at the expense of their pathological functions may uncover other novel macrophage reprogramming strategies that could be harnessed to reduce the global burden of chronic liver disease.

MATERIALS AND METHODS

CSF1-Fc reagents

This study used two CSF1-Fc reagents with equivalent biological impacts. The original porcine (P)-CSF1-Fc reagent was used at 1 mg/kg as in previous reports (Gow et al., 2014; Irvine et al., 2020; Sauter et al., 2016). The novel human CSF1-mouse Fc conjugate (HM-CSF1-Fc) was used at 5 mg/kg, as this dose elicited increased circulating monocytes, liver and spleen weight similar to 1 mg/kg P-CSF1-Fc. We used 1 mg/kg HM-CSF1-Fc as a sub-maximal dose in the setting of PHx (Figs 7, 8), as this dose induced liver growth without monocytosis (Fig. S2A-C). Pig and human CSF1 proteins are both active on mouse CSF1R (Gow et al., 2012) and in our hands the Fc conjugates have similar activity on mouse bone marrow (not shown). The difference in efficacy may reflect different pharmacokinetics. Pig immunoglobulin does not bind to human Fc receptors (Shields et al., 2001) and the pig IgG1A Fc fragment used (Gow et al., 2014) is completely divergent in the crucial FcR binding domain defined by site-directed mutagenesis (Egli et al., 2019) that is shared by mouse and human immunoglobulins. The mouse Fc domain used herein has the L234A/L235A mutations that reduce but do not abolish binding to mouse FcR and to C1q (Arduin et al., 2015).

Animals

Studies were approved by a University of Queensland animal ethics committee. The 6- to 8-week-old C57Bl6/J mice were sourced from the Animal Resource Centre (Perth, Australia) and housed in a specific pathogen-free facility. Animals were randomly assigned to CSF1-Fc and saline treatment groups, with mixed treatments in individual cages. For induction of liver fibrosis 300 mg/l TAA (Sigma-Aldrich) was added to the sole source of drinking water. CSF1-Fc was administered by sub-cutaneous injection. At sacrifice, blood was collected by cardiac puncture for haematology analysis (Mindray BC-5000) and serum separation (biochemical analysis by the University of Queensland Veterinary Laboratory Services).

Partial hepatectomy

Mice were anaesthetised by isoflurane inhalation. When fully anaesthetised, the mouse was placed supine on a warming pad. A 1.5 cm upper midline incision was made. After the liver and the ligamentum falciforme were exposed, the ligamentum was divided to the level of the superior vena cava to loosen the liver from the diaphragm. To achieve 50% PHx the left lateral and left median lobes were removed. The liver lobes to be resected were gently moved using saline-moistened cotton buds. A 5/0 suture was positioned around the appropriate lobe as near as possible to its base and tied with three knots. The lobe was removed distal to the suture, leaving a short tissue stem. The resected lobes were retained and analysed as the pre-PHx baseline histology. Following surgery, the abdominal cavity was rinsed with saline and the incision and skin were closed with a coated polyglactin 4/0 suture. The wound was disinfected, and the lost fluids were replaced by subcutaneous injection of up to 1 ml sterile saline. Mice were injected twice daily with buprenorphine for pain relief.

Histology

Livers were fixed in 4% paraformaldehyde and paraffin-embedded. For immunostaining, epitope retrieval was performed in Diva Decloaker (Biocare Medical) followed by staining for Ki67 (Abcam, ab16667, lot GR3313195-28, 1:100), F4/80 (Novus, NB600-404, Clone CI-A3-1, 1:400), wide-spectrum keratin [CKWSS, which labels bile duct epithelium and hepatic progenitor cells (Dako, Z0622, lot 10070520, 1:400)] or SMA (Dako, M0851, clone 1A4, 1:200). Secondary detection was with DAKO Envision HRP reagents or anti-species fluorophore conjugates [Thermo Fisher Scientific, goat anti-mouse AF488, A11029 (1:200); Abcam, donkey anti-rat AF647, ab150151 (1:200)]. Image quantification was performed from whole-slide digital images (VS120 scanner, Olympus) using ImageJ or Visiopharm software.

Flow cytometry

Liver non-parenchymal cells were isolated as previously described (Melino et al., 2016). Briefly, tissue disaggregation was performed by finely chopping liver samples (~1-2 g) in 10 ml digestion solution containing 1 mg/ml Collagenase IV (Worthington) and 20 µg/ml DNAse1 (Roche) and incubating at 37°C for 45 min on a rocking platform before mashing through a 70 µm filter (Falcon). The cell pellet was collected by centrifugation (400 ***g***) and resuspended in an isotonic 30% Percoll solution to separate hepatocytes and non-parenchymal cells. Cells were stained for a panel of myeloid markers [F4/80-AF647 (1:150), Cd11b-BV510 (1:200), Ly6G-BV785 (1:200), MHCII-BV421 (1:200), Tim4-PE-Cy7 (1:300), Ly6C-PE (1:300) (Biolegend)] in buffer containing 2.4G2 supernatant to block Fc binding, washed and resuspended in buffer containing viability dye 7AAD (Life Technologies) for acquisition using a Cytoflex (Becton Dickinson). Live single cells were identified for phenotypic analysis by excluding doublets (FSC-A>FSC-H), 7AAD+ dead cells and debris. Single colour controls were used for compensation and unstained and fluorescence-minus-one controls were used to confirm gating. Data were analysed using FlowJo 10 (Tree Star). Cell counts were calculated by multiplying the frequency of the cell type of interest by the total mononuclear cell yield/g of disaggregated tissue.

qPCR

Liver samples were collected in TRIzol (Sigma-Aldrich) for RNA extraction and cDNA synthesis (Bioline) according to manufacturer instructions. RT-PCR was performed using the SYBR Select Master Mix (Thermo Fisher Scientific) on an Applied Biosystems QuantStudio system. Primer pairs used in this study are as follows: *Hprt* F, 5′-GCAGTACAGCCCCAAAATGG-3′, *Hprt* R, 5′-AACAAAGTCTGGCCTGTATCCAA-3′; *Tbp* F, 5′-CTCAGTTACAGGTGGCAGCA-3′, *Tbp* R, 5′-ACCAACAATCACCAACAGCA-3′; *Adgre1* F, 5′-CTGTCTGCTCAACCGTCAGGTA-3′, *Adgre1* R, 5′-AGAAGTCTGGGAATGGGAGCTAA-3′; *Ccl2* F, 5′-CAAGATGATCCCAATGAGTAGGC-3′, *Ccl2* R, 5′-CTCTTGAGCTTGGTGACAAAAACTA-3′; *Ccr2* F, 5′-GAACTTGAATCATCTGCAAAAACAAAT-3′, *Ccr2* R, 5′-GGCAGGATCCAAGCTCCAAT-3′; *Acta2* F, 5′-GATCCTGACTGAGCGTGGCTAT-3′, *Acta2* R, 5′-CGTGGCCATCTCATTTTCAAAG-3′; *Col1a1* F, 5′-AGGGATCCAACGAGATCGAG-3′, *Col1a1* R, 5′-CAAGTTCCGGTGTGACTCGT-3′; *Col3a1* F, 5′-TGGGATCAAATGAAGGCGAAT-3′, *Col3a1* R, 5′-GCTCCATTCCCCAGTGTGTTTAG-3′; *Mmp9* F, 5′-AGGGGCGTGTCTGGAGATTC-3′, *Mmp9* R, 5′-TCCAGGGCACACCAGAGAAC-3′; *Mmp13* F, 5′-ACAAAGATTATCCCCGCCTCAT-3′, *Mmp13* R, 5′-GGCCCATTGAAAAAGTAGATATAGCC-3′; *Plau* F, 5′-GGCTTTGGAAAAGAGTCTGAAAGTG-3′, *Plau* R, 5′-GCCATAGTAGTGGGGCTGCAT-3′; *Tgfb1* F, 5′-GTGGCTGAACCAAGGAGACG-3′, *Tgfb1* R, 5′-GGCTGATCCCGTTGATTTCC-3′; *Hbegf* F, 5′-CTGAGGAGGACCTGAGCTATAGGA-3′, *Hbegf* R, 5′-GTTTTCATGGCTGCTGGTGA-3′; *Hgf* F, 5′-ATTGGATCAGGACCATGTGAGG-3′, *Hgf* R, 5′-CACATCCACGACCAGGAACA-3′; *Il6* F, 5′-AAATCGTGGAAATGAGAAAAGAGTTG-3′, *Il6* R, 5′-GCATCCATCATTTCTTTGTATCTCTG-3′; *Tnf* F, 5′-GGTCCCCAAAGGGATGAGAAG-3′, *Tnf* R, 5′-TCGAATTTTGAGAAGATGATCTGAGTG-3′; *Brg1* F, 5′-GAAAGTGGCTCTGAAGAGGAGG-3′, *Brg1* R, 5′-TCCACCTCAGAGACATCATCGC-3′.

Doppler imaging

Hepatic blood flow was assessed by Power Doppler imaging using a Vevo 2100 ultrasound system fitted with a MS250 transducer (20 MHz centre frequency; Fujifilm Visualsonics). Scan settings were pulse repetition frequency (PRF) at 3 KHz, Doppler gain at 37 dB, medium persistence (frame averaging), and scan distance of ∼20 mm, with a step size of 0.150 mm. Calculation of liver percent vascularity (PV) and 3D image reconstruction were achieved using Vevolab analysis software v5.5.1.

Data analysis

Sample sizes were determined by previous experiments using CSF1-Fc treatment that detected statistically significant impacts on liver growth and regeneration in healthy mice and acute injury models, as well as our previous experience with the TAA model of liver fibrosis (Gow et al., 2014; Irvine et al., 2020, 2015; Melino et al., 2016; Stutchfield et al., 2015). Analysis of histological and flow cytometry outcome data was performed blinded to treatment group. Data are presented as mean±s.d. Statistical tests were performed using GraphPad Prism 7.03. Data normality was tested using the Shapiro-Wilk test; unless otherwise stated, ordinary one-way ANOVA with Sidak's multiple comparisons testing was used. All tests were two-tailed. All authors had access to the study data and reviewed and approved the final manuscript.

Acknowledgements

K.M.I. and D.A.H. are grateful for core laboratory support from the Mater Foundation. We appreciate the support of the Preclinical Imaging, Biological Resources, Histology, Microscopy and Flow Cytometry Core Facilities at the Translational Research Institute.

Competing interests

The authors declare no competing or financial interests.

Author contributions

Conceptualization: S.K., B.G., E.E.P., D.A.H., K.M.I.; Methodology: S.K., B.G., B.W.C.T., K.A.S., G.M., A.D.C., E.E.P., K.M.I.; Formal analysis: S.K., B.G., G.M., K.M.I.; Investigation: S.K., B.G., N.T., M.C., M.F.C., O.L.P., B.W.C.T., K.A.S., A.R.P., K.M.I.; Resources: H.E., J.J.; Writing - original draft: D.A.H., K.M.I.; Writing - review & editing: S.K., B.G., N.T., M.C., M.F.C., D.L.P., B.W.C.T., K.A.S., H.E., J.J., K.P.A.M., G.M., G.A.R., A.R.P., A.D.C., E.E.P., D.A.H., K.M.I.; Visualization: S.K., B.W.C.T., K.A.S., K.M.I.; Supervision: G.A.R., D.A.H., K.M.I.; Project administration: K.M.I.; Funding acquisition: D.A.H., K.M.I.

Funding

This work was supported by the National Health and Medical Research Council (grant APP1162171 to K.M.I., D.A.H. and A.D.C.), and by core laboratory funding from the Mater Foundation (D.A.H., K.M.I.). Open access funding provided by University of Queensland. Deposited in PMC for immediate release.

References

Arduin, E., Arora, S., Bamert, P. R., Kuiper, T., Popp, S., Geisse, S., Grau, R., Calzascia, T., Zenke, G. and Kovarik, J. (2015). Highly reduced binding to high and low affinity mouse Fc gamma receptors by L234A/L235A and N297A Fc mutations engineered into mouse IgG2a. *Mol. Immunol.* **63**, 456-463. doi:10.1016/j.molimm.2014.09.017

Artru, F., Louvet, A. and Mathurin, P. (2017). Liver transplantation for patients with alcoholic hepatitis. *Liver Int.* **37**, 337-339. doi:10.1111/liv.13248

Asrani, S. K., Devarbhavi, H., Eaton, J. and Kamath, P. S. (2019). Burden of liver diseases in the world. *J. Hepatol.* **70**, 151-171. doi:10.1016/j.jhep.2018.09.014

Baker, G. R. and Levin, J. (1998). Transient thrombocytopenia produced by administration of macrophage colony-stimulating factor: investigations of the mechanism. *Blood* **91**, 89-99. doi:10.1182/blood.V91.1.89

Balkan, J., Doğğru-Abbasoğlul, S., Kanbagli, O., Çevikbas, U., Aykaç-Toker, G. and Uysal, M. (2001). Taurine has a protective effect against thioacetamide-induced liver cirrhosis by decreasing oxidative stress. *Hum. Exp. Toxicol.* **20**, 251-254. doi:10.1191/096032701678227758

Barcena, C., Aran, G., Perea, L., Sanjurjo, L., Tellez, E., Oncins, A., Masnou, H., Serra, I., Garcia-Gallo, M., Kremer, L. et al. (2019). CD5L is a pleiotropic player in liver fibrosis controlling damage, fibrosis and immune cell content. *EBioMedicine* **43**, 513-524. doi:10.1016/j.ebiom.2019.04.052

Bartocci, A., Mastrogiannis, D. S., Migliorati, G., Stockert, R. J., Wolkoff, A. W. and Stanley, E. R. (1987). Macrophages specifically regulate the concentration of their own growth factor in the circulation. *Proc. Natl. Acad. Sci. USA* **84**, 6179-6183. doi:10.1073/pnas.84.17.6179

Batoon, L., Millard, S. M., Raggatt, L. J., Sandrock, C. J., Pickering, E., Williams, K., Sun, L. W. H., Wu, A. C., Irvine, K. M., Pivonka, P. et al. (2021). Treatment with a long-acting chimeric CSF1 molecule enhances fracture healing of healthy and osteoporotic bones. *Biomaterials* **275**, 120936. doi:10.1016/j.biomaterials.2021.120936

Bird, T. G., Lu, W.-Y., Boulter, L., Gordon-Keylock, S., Ridgway, R. A., Williams, M. J., Taube, J., Thomas, J. A., Wojtacha, D., Gambardella, A. et al. (2013). Bone marrow injection stimulates hepatic ductular reactions in the absence of injury via macrophage-mediated TWEAK signaling. *Proc. Natl. Acad. Sci. USA* **110**, 6542-6547. doi:10.1073/pnas.1302168110

Bueno, M., Salgado, S., Beas-Zárate, C. and Armendariz-Borunda, J. (2006). Urokinase-type plasminogen activator gene therapy in liver cirrhosis is mediated by collagens gene expression down-regulation and up-regulation of MMPs, HGF and VEGF. *J. Gene Med.* **8**, 1291-1299. doi:10.1002/jgm.961

D'Ambrosio, R., Aghemo, A., Rumi, M. G., Ronchi, G., Donato, M. F., Paradis, V., Colombo, M. and Bedossa, P. (2012). A morphometric and immunohistochemical study to assess the benefit of a sustained virological response in hepatitis C virus patients with cirrhosis. *Hepatology* **56**, 532-543. doi:10.1002/hep.25606

Delire, B., Starkel, P. and Leclercq, I. (2015). Animal models for fibrotic liver diseases: what we have, what we need, and what is under development. *J. Clin. Transl. Hepatol.* **3**, 53-66. doi:10.14218/JCTH.2014.00035

Denny, W. A. and Flanagan, J. U. (2021). Small-molecule CSF1R kinase inhibitors; review of patents 2015-present. *Expert Opin. Ther. Pat.* **31**, 107-117. doi:10.1080/13543776.2021.1839414

Duffield, J. S., Forbes, S. J., Constandinou, C. M., Clay, S., Partolina, M., Vuthoori, S., Wu, S., Lang, R. and Iredale, J. P. (2005). Selective depletion of macrophages reveals distinct, opposing roles during liver injury and repair. *J. Clin. Invest.* **115**, 56-65. doi:10.1172/JCI200522675

Dwyer, B. J., Macmillan, M. T., Brennan, P. N. and Forbes, S. J. (2021). Cell therapy for advanced liver diseases: repair or rebuild. *J. Hepatol.* **74**, 185-199. doi:10.1016/j.jhep.2020.09.014

Egli, J., Schlothauer, T., Spick, C., Seeber, S., Singer, T., Odermatt, A. and Iglesias, A. (2019). The binding of human IgG to minipig FcgammaRs - implications for preclinical assessment of therapeutic antibodies. *Pharm. Res.* **36**, 47. doi:10.1007/s11095-019-2574-y

Garnick, M. B. and O'Reilly, R. J. (1989). Clinical promise of new hematopoietic growth factors: M-CSF, IL-3, IL-6. *Hematol. Oncol. Clin. North Am.* **3**, 495-509. doi:10.1016/S0889-8588(18)30544-6

Gow, D. J., Garceau, V., Kapetanovic, R., Sester, D. P., Fici, G. J., Shelly, J. A., Wilson, T. L. and Hume, D. A. (2012). Cloning and expression of porcine Colony Stimulating Factor-1 (CSF-1) and Colony Stimulating Factor-1 Receptor (CSF-1R) and analysis of the species specificity of stimulation by CSF-1 and Interleukin 34. *Cytokine* **60**, 793-805. doi:10.1016/j.cyto.2012.08.008

Gow, D. J., Sauter, K. A., Pridans, C., Moffat, L., Sehgal, A., Stutchfield, B. M., Raza, S., Beard, P. M., Tsai, Y. T., Bainbridge, G. et al. (2014). Characterisation of a novel Fc conjugate of macrophage colony-stimulating factor. *Mol. Ther.* **22**, 1580-1592. doi:10.1038/mt.2014.112

Grabert, K., Sehgal, A., Irvine, K. M., Wollscheid-Lengeling, E., Ozdemir, D. D., Stables, J., Luke, G. A., Ryan, M. D., Adamson, A., Humphreys, N. E. et al. (2020). A transgenic line that reports CSF1R protein expression provides a definitive marker for the mouse mononuclear phagocyte system. *J. Immunol.* **205**, 3154-3166. doi:10.4049/jimmunol.2000835

Hackl, C., Schlitt, H. J., Renner, P. and Lang, S. A. (2016). Liver surgery in cirrhosis and portal hypertension. *World J. Gastroenterol.* **22**, 2725-2735. doi:10.3748/wjg.v22.i9.2725

Hamilton, J. A., Cook, A. D. and Tak, P. P. (2016). Anti-colony-stimulating factor therapies for inflammatory and autoimmune diseases. *Nat. Rev. Drug Discov.* **16**, 53-70. doi:10.1038/nrd.2016.231

Han, Y.-H., Shin, K.-O., Kim, J.-Y., Khadka, D. B., Kim, H.-J., Lee, Y.-M., Cho, W.-J., Cha, J.-Y., Lee, B.-J. and Lee, M.-O. (2019). A maresin 1/RORalpha/12-lipoxygenase autoregulatory circuit prevents inflammation and progression of nonalcoholic steatohepatitis. *J. Clin. Invest.* **129**, 1684-1698. doi:10.1172/JCI124219

Holczbauer, A., Wangensteen, K. J. and Shin, S. (2021). Cellular origins of regenerating liver and hepatocellular carcinoma. *JHEP Rep.* **4**, 100416. doi:10.1016/j.jhepr.2021.100416.

Hosseini, N., Shor, J. and Szabo, G. (2019). Alcoholic hepatitis: a review. *Alcohol Alcohol.* **54**, 408-416. doi:10.1093/alcalc/agz036

Hume, D. A. and MacDonald, K. P. A. (2012). Therapeutic applications of macrophage colony-stimulating factor-1 (CSF-1) and antagonists of CSF-1 receptor (CSF-1R) signaling. *Blood* **119**, 1810-1820. doi:10.1182/blood-2011-09-379214

Hume, D. A., Irvine, K. M. and Pridans, C. (2019). The mononuclear phagocyte system: the relationship between monocytes and macrophages. *Trends Immunol.* **40**, 98-112. doi:10.1016/j.it.2018.11.007

Irvine, K. M., Clouston, A. D., Gadd, V. L., Miller, G. C., Wong, W.-Y., Melino, M., Maradana, M. R., MacDonald, K., Lang, R. A., Sweet, M. J. et al. (2015). Deletion of Wntless in myeloid cells exacerbates liver fibrosis and the ductular

reaction in chronic liver injury. *Fibrogen. Tissue Repair* **8**, 19. doi:10.1186/s13069-015-0036-7

Irvine, K. M., Ratnasekera, I., Powell, E. E. and Hume, D. A. (2019). Causes and consequences of innate immune dysfunction in cirrhosis. *Front. Immunol.* **10**, 293. doi:10.3389/fimmu.2019.00293

Irvine, K. M., Caruso, M., Cestari, M. F., Davis, G. M., Keshvari, S., Sehgal, A., Pridans, C. and Hume, D. A. (2020). Analysis of the impact of CSF-1 administration in adult rats using a novel Csf1r-mApple reporter gene. *J. Leukoc. Biol.* **107**, 221-235. doi:10.1002/JLB.MA0519-149R

Jakubowski, A. A., Bajorin, D. F., Templeton, M. A., Chapman, P. B., Cody, B. V., Thaler, H., Tao, Y., Filippa, D. A., Williams, L., Sherman, M. L. et al. (1996). Phase I study of continuous-infusion recombinant macrophage colony-stimulating factor in patients with metastatic melanoma. *Clin. Cancer Res.* **2**, 295-302.

Kiso, S., Kawata, S., Tamura, S., Inui, Y., Yoshida, Y., Sawai, Y., Umeki, S., Ito, N., Yamada, A., Miyagawa, J. et al. (2003). Liver regeneration in heparin-binding EGF-like growth factor transgenic mice after partial hepatectomy. *Gastroenterology* **124**, 701-707. doi:10.1053/gast.2003.50097

Kisseleva, T. and Brenner, D. (2021). Molecular and cellular mechanisms of liver fibrosis and its regression. *Nat. Rev. Gastroenterol. Hepatol.* **18**, 151-166. doi:10.1038/s41575-020-00372-7

Konishi, T., Schuster, R. M., Goetzman, H. S., Caldwell, C. C. and Lentsch, A. B. (2020). Fibrotic liver has prompt recovery after ischemia-reperfusion injury. *Am. J. Physiol. Gastrointest. Liver Physiol.* **318**, G390-G400. doi:10.1152/ajpgi.00137.2019

Krenzien, F., Schmelzle, M., Struecker, B., Raschzok, N., Benzing, C., Jara, M., Bahra, M., Öllinger, R., Sauer, I. M., Pascher, A. et al. (2018). Liver transplantation and liver resection for cirrhotic patients with hepatocellular carcinoma: comparison of long-term survivals. *J. Gastrointest. Surg.* **22**, 840-848. doi:10.1007/s11605-018-3690-4

Kuramitsu, K., Sverdlov, D. Y., Liu, S. B., Csizmadia, E., Burkly, L., Schuppan, D., Hanto, D. W., Otterbein, L. E. and Popov, Y. (2013). Failure of fibrotic liver regeneration in mice is linked to a severe fibrogenic response driven by hepatic progenitor cell activation. *Am. J. Pathol.* **183**, 182-194. doi:10.1016/j.ajpath.2013.03.018

Lemoinne, S. and Friedman, S. L. (2019). New and emerging anti-fibrotic therapeutics entering or already in clinical trials in chronic liver diseases. *Curr. Opin. Pharmacol.* **49**, 60-70. doi:10.1016/j.coph.2019.09.006

Li, L., Wei, W., Li, Z., Chen, H., Li, Y., Jiang, W., Chen, W., Kong, G., Yang, J. and Li, Z. (2018). The spleen promotes the secretion of CCL2 and supports an M1 dominant phenotype in hepatic macrophages during liver fibrosis. *Cell. Physiol. Biochem.* **51**, 557-574. doi:10.1159/000495276

Liu, X., Xu, J., Rosenthal, S., Zhang, L.-J., McCubbin, R., Meshgin, N., Shang, L., Koyama, Y., Ma, H.-Y., Sharma, S. et al. (2020). Identification of lineage-specific transcription factors that prevent activation of hepatic stellate cells and promote fibrosis resolution. *Gastroenterology* **158**, 1728-1744.e14. doi:10.1053/j.gastro.2020.01.027

Lodder, J., Denaës, T., Chobert, M.-N., Wan, J. H., El-Benna, J., Pawlotsky, J.-M., Lotersztajn, S. and Teixeira-Clerc, F. (2015). Macrophage autophagy protects against liver fibrosis in mice. *Autophagy* **11**, 1280-1292. doi:10.1080/15548627.2015.1058473

Ludin, A., Itkin, T., Gur-Cohen, S., Mildner, A., Shezen, E., Golan, K., Kollet, O., Kalinkovich, A., Porat, Z., D'Uva, G. et al. (2012). Monocytes-macrophages that express alpha-smooth muscle actin preserve primitive hematopoietic cells in the bone marrow. *Nat. Immunol.* **13**, 1072-1082. doi:10.1038/ni.2408

Marcellin, P., Gane, E., Buti, M., Afdhal, N., Sievert, W., Jacobson, I. M., Washington, M. K., Germanidis, G., Flaherty, J. F., Aguilar Schall, R. A. et al. (2013). Regression of cirrhosis during treatment with tenofovir disoproxil fumarate for chronic hepatitis B: a 5-year open-label follow-up study. *Lancet* **381**, 468-475. doi:10.1016/S0140-6736(12)61425-1

Mehal, W. Z., Azzaroli, F. and Crispe, I. N. (2001). Immunology of the healthy liver: old questions and new insights. *Gastroenterology* **120**, 250-260. doi:10.1053/gast.2001.20947

Melgar-Lesmes, P., Luquero, A., Parra-Robert, M., Mora, A., Ribera, J., Edelman, E. R. and Jiménez, W. (2018). Graphene-dendrimer nanostars for targeted macrophage overexpression of metalloproteinase 9 and hepatic fibrosis precision therapy. *Nano Lett.* **18**, 5839-5845. doi:10.1021/acs.nanolett.8b02498

Melino, M., Gadd, V. L., Alexander, K. A., Beattie, L., Lineburg, K. E., Martinez, M., Teal, B., Le Texier, L., Irvine, K. M., Miller, G. C. et al. (2016). Spatiotemporal characterization of the cellular and molecular contributors to liver fibrosis in a murine hepatotoxic-injury model. *Am. J. Pathol.* **186**, 524-538. doi:10.1016/j.ajpath.2015.10.029

Meza-Rios, A., Garcia-Benavides, L., Garcia-Banuelos, J., Salazar-Montes, A., Armendariz-Borunda, J. and Sandoval-Rodriguez, A. (2016). Simultaneous administration of ADSCs-based therapy and gene therapy using Ad-huPA reduces experimental liver fibrosis. *PLoS ONE* **11**, e0166849. doi:10.1371/journal.pone.0166849

Michalopoulos, G. K. and Bhushan, B. (2021). Liver regeneration: biological and pathological mechanisms and implications. *Nat. Rev. Gastroenterol. Hepatol.* **18**, 40-55. doi:10.1038/s41575-020-0342-4

Mitchell, O., Feldman, D. M., Diakow, M. and Sigal, S. H. (2016). The pathophysiology of thrombocytopenia in chronic liver disease. *Hepatic Med. Evidence Res.* **8**, 39-50. doi:10.2147/HMER.S74612

Miyaoka, Y., Ebato, K., Kato, H., Arakawa, S., Shimizu, S. and Miyajima, A. (2012). Hypertrophy and unconventional cell division of hepatocytes underlie liver regeneration. *Curr. Biol.* **22**, 1166-1175. doi:10.1016/j.cub.2012.05.016

Moon, A. M., Singal, A. G. and Tapper, E. B. (2020). Contemporary epidemiology of chronic liver disease and cirrhosis. *Clin. Gastroenterol. Hepatol.* **18**, 2650-2666. doi:10.1016/j.cgh.2019.07.060

Mooney, J. E., Rolfe, B. E., Osborne, G. W., Sester, D. P., van Rooijen, N., Campbell, G. R., Hume, D. A. and Campbell, J. H. (2010). Cellular plasticity of inflammatory myeloid cells in the peritoneal foreign body response. *Am. J. Pathol.* **176**, 369-380. doi:10.2353/ajpath.2010.090545

Nakano, Y., Nakao, S., Sumiyoshi, H., Mikami, K., Tanno, Y., Sueoka, M., Kasahara, D., Kimura, H., Moro, T., Kamiya, A. et al. (2017). Identification of a novel alpha-fetoprotein-expressing cell population induced by the Jagged1/Notch2 signal in murine fibrotic liver. *Hepatol. Commun.* **1**, 215-229. doi:10.1002/hep4.1026

Perugorria, M. J., Esparza-Baquer, A., Oakley, F., Labiano, I., Korosec, A., Jais, A., Mann, J., Tiniakos, D., Santos-Laso, A., Arbelaiz, A. et al. (2018). Non-parenchymal TREM-2 protects the liver from immune-mediated hepatocellular damage. *Gut* **68**, 533-546. doi:10.1136/gutjnl-2017-314107

Popov, Y., Sverdlov, D. Y., Sharma, A. K., Bhaskar, K. R., Li, S., Freitag, T. L., Lee, J., Dieterich, W., Melino, G. and Schuppan, D. (2011). Tissue transglutaminase does not affect fibrotic matrix stability or regression of liver fibrosis in mice. *Gastroenterology* **140**, 1642-1652. doi:10.1053/j.gastro.2011.01.040

Ramachandran, P., Pellicoro, A., Vernon, M. A., Boulter, L., Aucott, R. L., Ali, A., Hartland, S. N., Snowdon, V. K., Cappon, A., Gordon-Walker, T. T. et al. (2012). Differential Ly-6C expression identifies the recruited macrophage phenotype, which orchestrates the regression of murine liver fibrosis. *Proc. Natl. Acad. Sci. USA* **109**, E3186-E3195. doi:10.1073/pnas.1119964109

Sakai, M., Troutman, T. D., Seidman, J. S., Ouyang, Z., Spann, N. J., Abe, Y., Ego, K. M., Bruni, C. M., Deng, Z., Schlachetzki, J. C. M. et al. (2019). Liver-derived signals sequentially reprogram myeloid enhancers to initiate and maintain Kupffer cell identity. *Immunity* **51**, 655-670.e8. doi:10.1016/j.immuni.2019.09.002

Salgado, S., Garcia, J., Vera, J., Siller, F., Bueno, M., Miranda, A., Segura, A., Grijalva, G., Segura, J., Orozco, H. et al. (2000). Liver cirrhosis is reverted by urokinase-type plasminogen activator gene therapy. *Mol. Ther.* **2**, 545-551. doi:10.1006/mthe.2000.0210

Sauter, K. A., Waddell, L. A., Lisowski, Z. M., Young, R., Lefevre, L., Davis, G. M., Clohisey, S. M., McCulloch, M., Magowan, E., Mabbott, N. A. et al. (2016). Macrophage colony-stimulating factor (CSF1) controls monocyte production and maturation and the steady-state size of the liver in pigs. *Am. J. Physiol. Gastrointest. Liver Physiol.* **311**, G533-G547. doi:10.1152/ajpgi.00116.2016

Schuppan, D., Surabattula, R. and Wang, X. Y. (2018). Determinants of fibrosis progression and regression in NASH. *J. Hepatol.* **68**, 238-250. doi:10.1016/j.jhep.2017.11.012

Seifert, L., Deutsch, M., Alothman, S., Alqunaibit, D., Werba, G., Pansari, M., Pergamo, M., Ochi, A., Torres-Hernandez, A., Levie, E. et al. (2015). Dectin-1 regulates hepatic fibrosis and hepatocarcinogenesis by suppressing TLR4 signaling pathways. *Cell Rep.* **13**, 1909-1921. doi:10.1016/j.celrep.2015.10.058

Shields, R. L., Namenuk, A. K., Hong, K., Meng, Y. G., Rae, J., Briggs, J., Xie, D., Lai, J., Stadlen, A., Li, B. et al. (2001). High resolution mapping of the binding site on human IgG1 for Fc gamma RI, Fc gamma RII, Fc gamma RIII, and FcRn and design of IgG1 variants with improved binding to the Fc gamma R. *J. Biol. Chem.* **276**, 6591-6604. doi:10.1074/jbc.M009483200

So, J., Kim, A., Lee, S.-H. and Shin, D. (2020). Liver progenitor cell-driven liver regeneration. *Exp. Mol. Med.* **52**, 1230-1238. doi:10.1038/s12276-020-0483-0

Stacey, K. J., Fowles, L. F., Colman, M. S., Ostrowski, M. C. and Hume, D. A. (1995). Regulation of urokinase-type plasminogen activator gene transcription by macrophage colony-stimulating factor. *Mol. Cell. Biol.* **15**, 3430-3441. doi:10.1128/MCB.15.6.3430

Stutchfield, B. M., Antoine, D. J., Mackinnon, A. C., Gow, D. J., Bain, C. C., Hawley, C. A., Hughes, M. J., Francis, B., Wojtacha, D., Man, T. Y. et al. (2015). CSF1 restores innate immunity after liver injury in mice and serum levels indicate outcomes of patients with acute liver failure. *Gastroenterology* **149**, 1896-1909.e14. doi:10.1053/j.gastro.2015.08.053

Stutchfield, B. M., Starkey Lewis, P., Wigmore, S., Simpson, K., Hume, D. and Forbes, S. J. (2021). Serum CSF1 levels are elevated in patients following partial hepatectomy and acetaminophen induced acute liver failure: reanalysis of previous data. *bioRxiv* doi:10.1101/2021.04.02.437789

Summers, K. M., Bush, S. J. and Hume, D. A. (2020). Network analysis of transcriptomic diversity amongst resident tissue macrophages and dendritic cells in the mouse mononuclear phagocyte system. *PLoS Biol.* **18**, e3000859. doi:10.1371/journal.pbio.3000859

Tacke, F. (2017). Targeting hepatic macrophages to treat liver diseases. *J. Hepatol.* **66**, 1300-1312. doi:10.1016/j.jhep.2017.02.026

Thomas, J. A., Pope, C., Wojtacha, D., Robson, A. J., Gordon-Walker, T. T., Hartland, S., Ramachandran, P., Van, D. M., Hume, D. A., Iredale, J. P. et al. (2011). Macrophage therapy for murine liver fibrosis recruits host effector cells improving fibrosis, regeneration, and function. *Hepatology* **53**, 2003-2015. doi:10.1002/hep.24315

Wan, J., Weiss, E., Ben Mkaddem, S., Mabire, M., Choinier, P. M., Picq, O., Thibault-Sogorb, T., Hegde, P., Pishvaie, D., Bens, M. et al. (2020). LC3-associated phagocytosis protects against inflammation and liver fibrosis via immunoreceptor inhibitory signaling. *Sci. Transl. Med.* **12**, eaaw8523. doi:10.1126/scitranslmed.aaw8523

Wang, B., Kaufmann, B., Engleitner, T., Lu, M., Mogler, C., Olsavszky, V., Öllinger, R., Zhong, S., Geraud, C., Cheng, Z. et al. (2019). Brg1 promotes liver regeneration after partial hepatectomy via regulation of cell cycle. *Sci. Rep.* **9**, 2320. doi:10.1038/s41598-019-38568-w

Williams, M. J., Clouston, A. D. and Forbes, S. J. (2014). Links between hepatic fibrosis, ductular reaction, and progenitor cell expansion. *Gastroenterology* **146**, 349-356. doi:10.1053/j.gastro.2013.11.034

Wynn, T. A. (2008). Cellular and molecular mechanisms of fibrosis. *J. Pathol.* **214**, 199-210. doi:10.1002/path.2277

Yada, A., Iimuro, Y., Uyama, N., Uda, Y., Okada, T. and Fujimoto, J. (2015). Splenectomy attenuates murine liver fibrosis with hypersplenism stimulating hepatic accumulation of Ly-6C(lo) macrophages. *J. Hepatol.* **63**, 905-916. doi:10.1016/j.jhep.2015.05.010

Zheng, Z., Wang, H., Li, L., Zhang, S., Zhang, C., Zhang, H., Ji, F., Liu, X., Zhu, K., Kong, G. et al. (2020). Splenectomy enhances the Ly6C(low) phenotype in hepatic macrophages by activating the ERK1/2 pathway during liver fibrosis. *Int. Immunopharmacol.* **86**, 106762. doi:10.1016/j.intimp.2020.106762

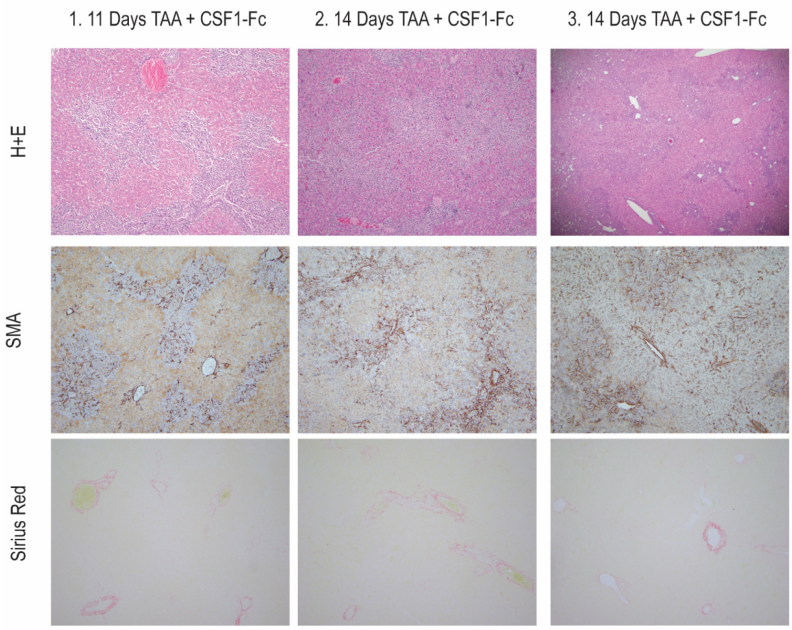

Fig. S1. Co-administration of CSF1-Fc and TAA exacerbated liver inflammation. Female C57/B16 mice were administered 300 mg/L TAA in drinking water in conjunction with bi-weekly treatment with 1 mg/kg pCSF1-Fc commencing on Day 1. Mice 1 and 2 died unexpectedly 11 and 14 days post commencement and mouse 3 was culled on day 14. Liver sections were stained with H+E, anti-SMA antibody or picrosirius red. 10 x magnification.

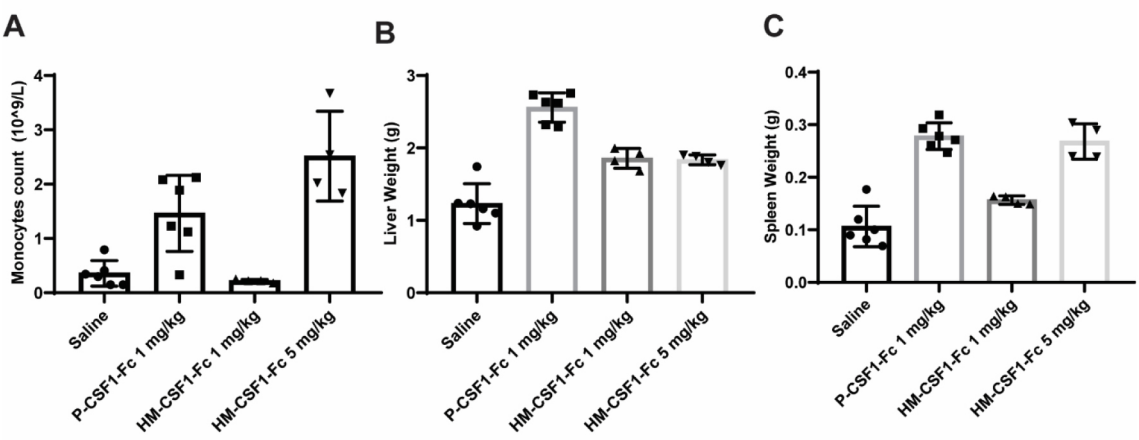

Fig. S2. Comparison of biological impacts of P-CSF-Fc and HM-CSF1-Fc. Male C57/Bl6 mice were administered 4 successive daily injections of porcine (P)-CSF1-Fc or a human CSF1-mouse Fe conjugate (HM-CSF1-Fc). (A) circulating monocyte count, (B) liver weight and (C) spleen weight at sacrifice.

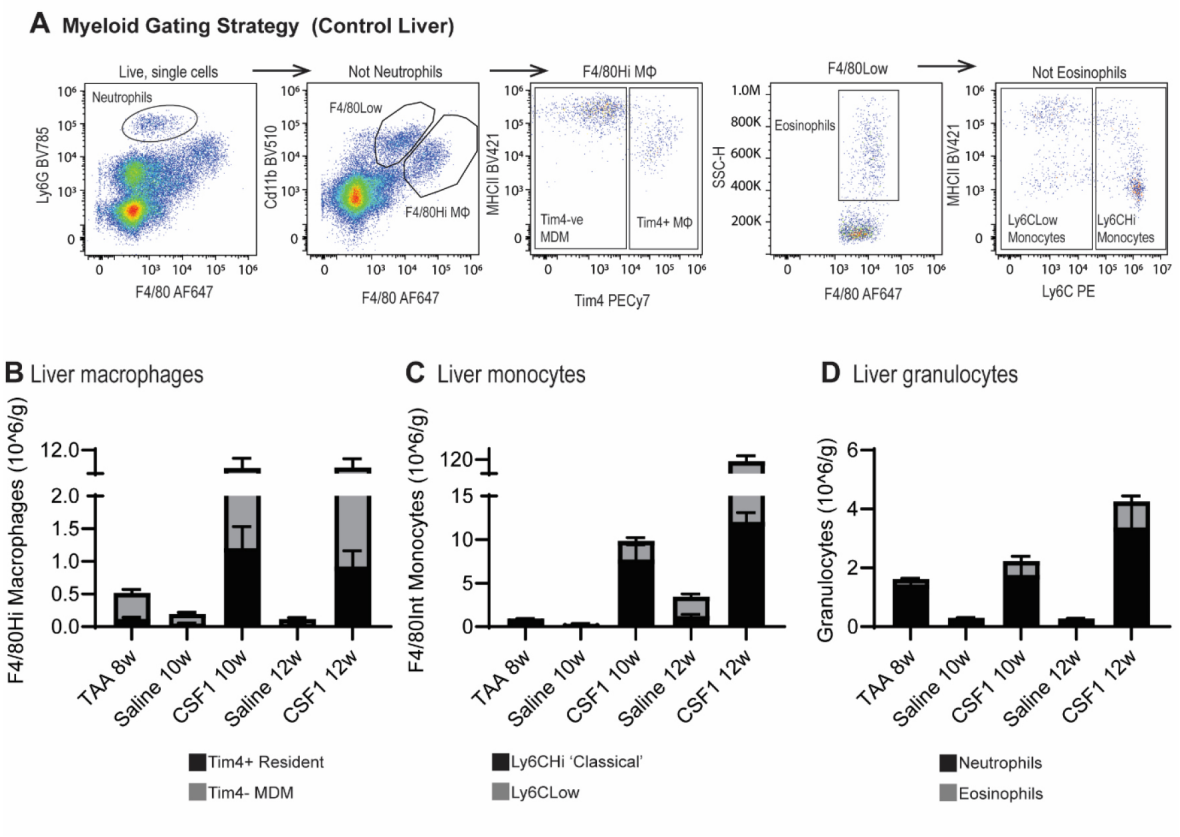

Fig. S3. CSF1-Fc treatment increases the abundance of hepatic classical and non-classical monocytes, monocyte-derived macrophages and kupffer cells during regression of TAA-induced fibrosis. Groups of 6 female mice were treated with TAA for 8 weeks, followed by bi-weekly treatment with 1 mg/kg P-CSF1-Fc for up to 4 weeks. Hepatic non-parenchymal cells were isolated from disaggregated livers for flow cytometry analysis at baseline (TAA 8w) or following 2 or 4 weeks CSF1-Fc treatment (CSF110w and 12w, respectively. (A) Myeloid cell ating strategy. Number of (B) nm4+ and Tim4-F4/80Hi macrophages, (C) Ly6CHi and Ly6Clow F4/801nt monocytes, (D) Ly6G+ neutrophils and F4/801nt/SSCHi eosinophils per gram of liver.

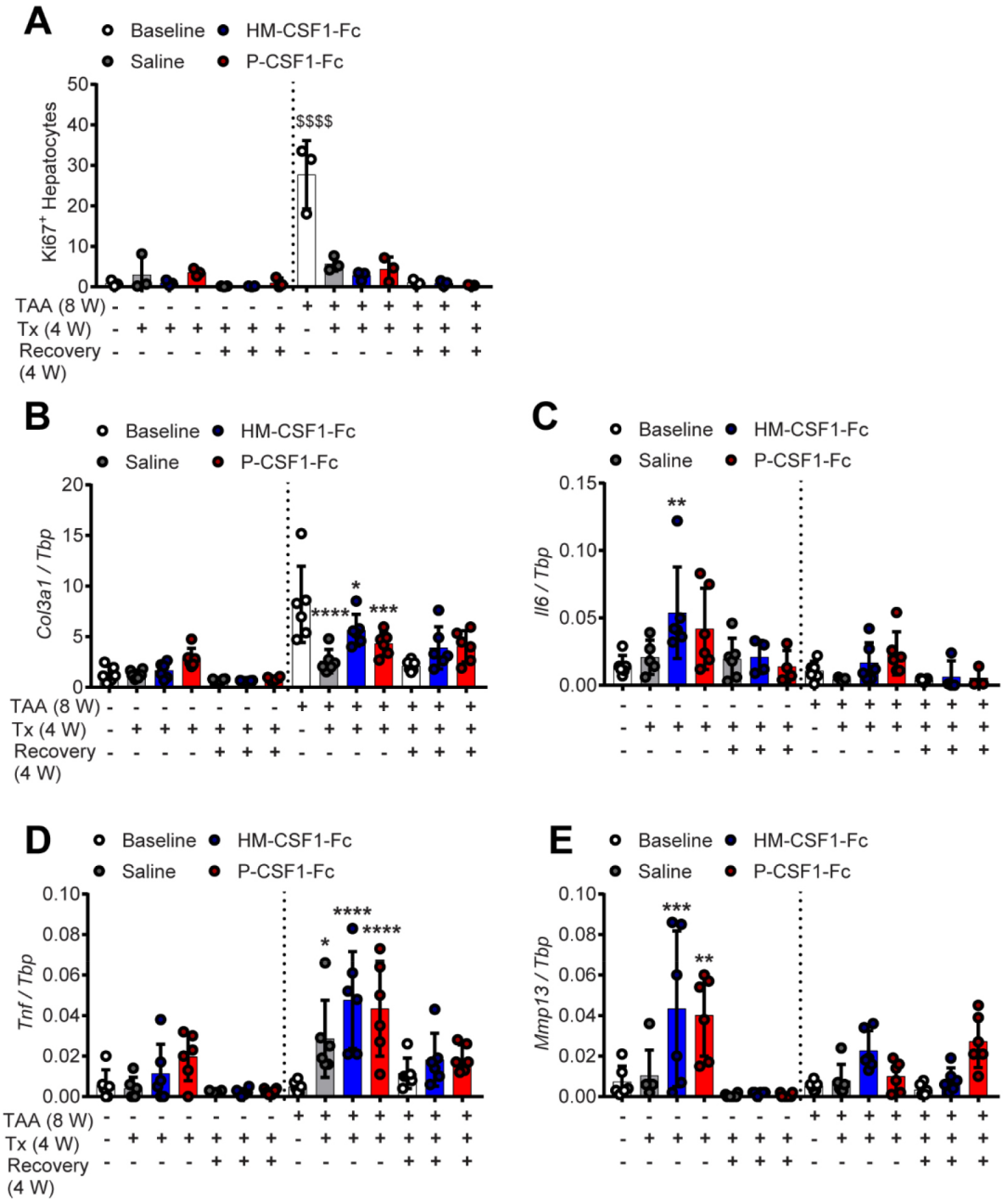

Fig. S4. Impacts of chronic CSFI-Fc treatment on hepatic gene expression. Experimental design as in Figure 1A. (A) Quantification of Ki67+ hepato-cytes by image analysis of IHC staining. Expression of Col3a 1 (B), 116 (C), Tnf (D), and Mmpl 3 (E) in whole liver was quantified by RT-PCR. One-Way ANOVA with multiple comparison, *p<0.05, **p<0.01, ***p<0.001, ****p<0.0001 comparing to baseline in same group.

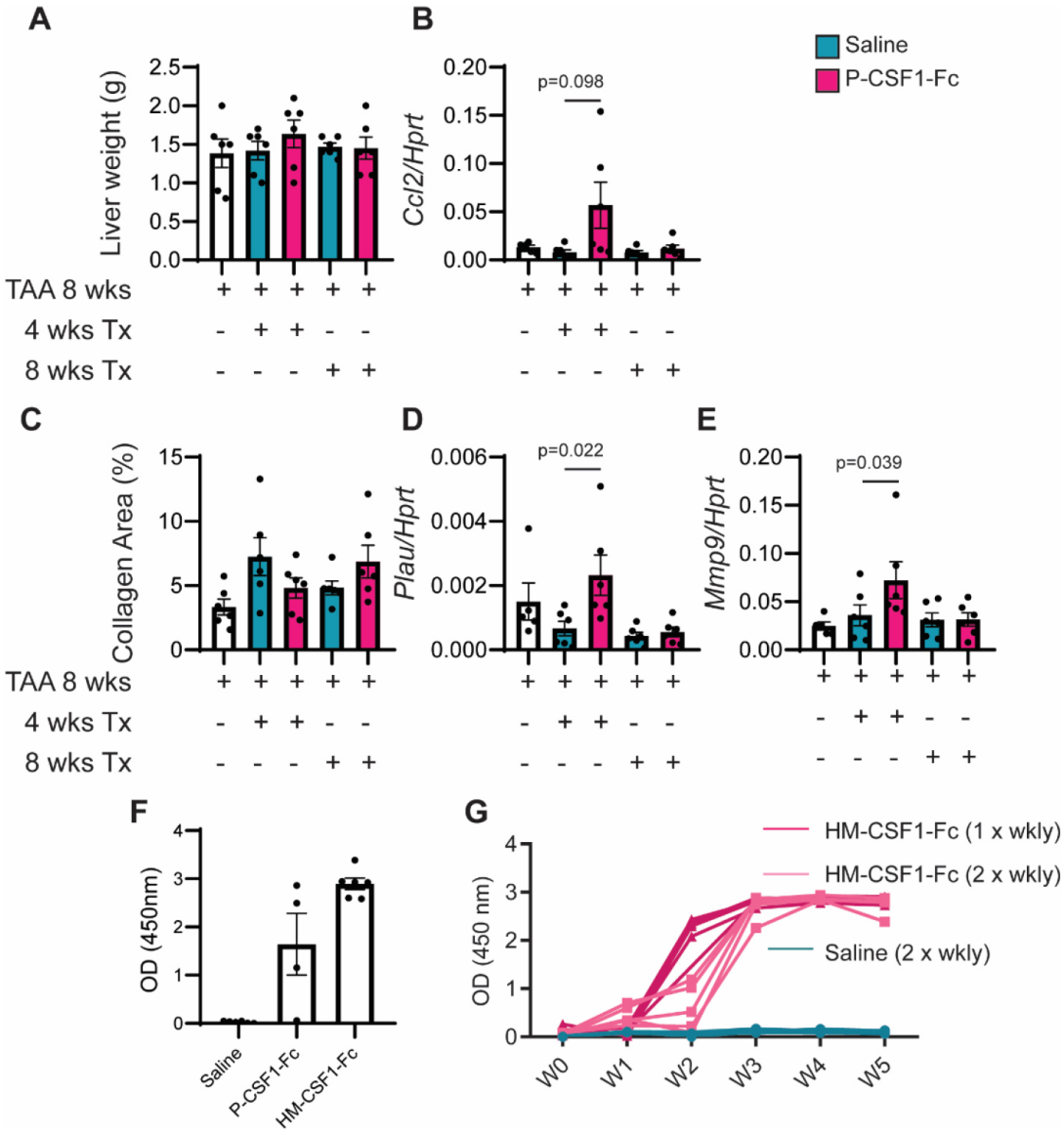

Fig. S5. Transient response to extended CSF1-Fc treatment is associated with anti-CSF1-Fc antibodies. Groups of 6 female C57/B16J mice were administered TAA in drinking water for 8 weeks, then returned to normal drinking water and treated with 1 mg/kg P-CSF1-Fc or saline control once weekly for 8 weeks. (A) Liver weight at sacrifice. Liver Ccl2 (b) and Adgre1 (?) mRNA expression. Liver fibrosis (collagen area) (C). Liver Plau (D) and Mmp9 (E) expression. Kruskal-Wallis, Dunn's multiple comparison test. (F) Mice were treated once weekly with P-CSF1-Fc or HM-CSF1-Fc for 4 weeks and serum antibodies to the respective CSF1-Fc reagent were detected by ELISA (1:1000 serum dilution). (G) Mice were treated once or twice weekly with HM-CSF1-Fc with weekly blood collection. Anti-CSF1-Fc antibodies in serum (1:1000 dilution) were detected by ELISA.